VACUOLAR H-ATPase AND THE NEPHRON: DEVELOPMENTAL APOPTOSIS AND ADULT PHYSIOLOGY

By

LISA M. CURTIS

A DISSERTATION PRESENTED TO THE GRADUATE SCHOOL
OF THE UNIVERSITY OF FLORIDA IN PARTIAL FULFILLMENT
OF THE REQUIREMENTS FOR THE DEGREE OF
DOCTOR OF PHILOSOPHY

UNIVERSITY OF FLORIDA

2001

Copyright 2001

by

Lisa M. Curtis

To Erin, Ryan and Genna:
The sky is the limit!

ACKNOWLEDGMENTS

I would like to sincerely thank my mentors, Dr. Kirsten Madsen and Dr. Stephen Gluck, as well as my committee members, Drs. Colin Sumners, Stephen Sugrue, Jill Verlander, John Aris, and Susan Frost, for their support and encouragement throughout my graduate program. I am also grateful to the American Heart Association and its generous donors for the two-year Graduate Fellowship Award, which supported me during these studies. I would also like to acknowledge the generous gift of several antibodies used in these studies, without which they could not have been completed: Dr. Steven J. Fluharty for the antibody to the AT_2R (Philadelphia, PA), Dr. Merino Zerial for the antibodies to Rab 18 and Rab 20 (EMBL, Germany), Dr. Kirsten Madsen and Dr. Paul Linser for the CAII antibody (UF). I would like to thank Dr. Jill Verlander for her dissection of the renal tubules and Ms. Wendy Wilbur for processing these tissues for the ELISA studies. I thank the entire Verlander lab for their amusing conversations. My gratitude goes to Dr. Martha Campbell-Thompson for always being available to help on the *in situ* hybridization studies, which unfortunately did not ultimately prove to be useful in my project. The preparation of kidneys from the HO-1 transgenic mice was done by Dr. Anupam Agarwal, Dr. Fumie Shiraishi and Ms. Leigh Truong. The sectioning of the developmental rats in the angiotensin studies was done by Ms. Melissa Lewis and Dr. Li Zhang. I am indebted to all of them for their excellent efforts and their friendship. I would like

to thank the members of the Gluck Lab Group for their discussions, scientific and otherwise, which made working in the lab more enjoyable. I would like to specifically mention Dr. Mark Segal for his suggestions and enthusiasm. Likewise, the encouragement of Drs. Ming Lu and Shannon Holliday were invaluable. I thank the administrative staff of the Department of Anatomy and Cell Biology, Joey Pelham, Lynda Hanssen, Todd Barnash and Ginger Wilson, and of the Division of Nephrology, Dawn Stewart and Linda Curry, for their help as well. I am grateful to the entire faculty of the Department of Anatomy and Cell Biology for their many suggestions and accessibility. I would like to express my gratitude to Dr. Kyle Rarey not only for his continual encouragement, but also for showing me that research is uniquely rewarding. I thank my friends, Nathalie, Matthew, Bonnie, John, Marcie, Bobbie and Lillie, for keeping me sane. Finally, I would like to thank my fiancé, my mom and dad, and my brothers and sisters, Martha, Louise, Byron, Robert, Barry and David, for their unending patience, encouragement and support.

TABLE OF CONTENTS

page

ACKNOWLEDGMENTS iv

ABBREVIATIONS ix

ABSTRACT x

CHAPTERS

1 INTRODUCTION 1

Kidney Development 1
Angiotensin II 3
Vacuolar H-ATPase 5
V-ATPase in Apoptosis 5
Structure and Function 6
Regulation 6
Rab GTPases 8
Rab 5a 11
Rab 11 12
Rab 13 13
Rab 18 13
Rab 20 14

2 MATERIALS AND METHODS 15

Angiotensin II Effects on Apoptosis 15
Animals 15
Developmental 15
Adult 15
Animal Treatments 16
ACE inhibitor 16
Receptor blockade 16
Antibodies and Reagents 16
Cell Culture 17
Cell Treatments 18
Serum starvation 18
Angiotensin II administration 18

Angiotensin II receptor blockade 18
Detection of Apoptotic Nuclei by TUNEL 19
Tissue sections 19
Cultured cells 20
Detection of Apoptotic Nuclei in Cultured Cells by Labeling of Annexin V and Propidium Iodide 21
Detection of Proliferating Cells by Immunolabeling of BrdU 21
Tissue sections 21
Cultured cells 22
ELISA 22
Rab GTPases in Mouse Kidney 23
Animals 23
Tissue Preparation for Immunolabeling 23
Imaging 24
Tissue Preparation for Immunoblotting 24
Antibodies and Reagents 24
Cell Culture 25
Immunostaining of Mouse Kidney 26
Enzyme immunostaining 26
Fluorescence immunohistochemistry 27
Detection of Rab GTPases in Mouse Tissues 28
SDS-PAGE 28
Immunoblotting 29
Generation of recombinant Rab 11 immunogen 30
Isolation of Mouse Kidney Fractions by Differential Centrifugation 31
Characterization of Mouse Kidney Fractions on Percoll Gradients 32

3 ANGIOTENSIN II EFFECTS ON APOPTOSIS 34

In vivo Studies 34
Establishment of Cell Proliferation and Cell Death Techniques 34
Cell proliferation 34
Cell death 34
Treatment of neonatal rat pups with an ACE inhibitor 36
Treatment of neonatal rat pups with an AT_1R or AT_2R blocker 36
In vitro Studies 38
Localization of the AT_1R in cultured cells by immunocytochemistry and AT_2R in microdissected tubules by ELISA 38
Evaluation of the response of mTAL and OMCD cells to treatment with Ang 39
Effects in mTAL and OMCD cells treated with Ang with and without blockade of either the AT_1R or the AT_2R 40

4 RAB GTPases AND V-ATPase IN ADULT MOUSE KIDNEY 42

Tissue- and cell-type specific distribution of Rab GTPases in the mouse kidney 42

Rab 5a 42
Rab 11 45
Rab 13 49
Rab 18 51
Rab 20 53
Co-fractionation of Rab GTPases with V-ATPase 57

5 CONCLUSIONS 62

Angiotensin II Effects on Apoptosis 62
Rab GTPases in Adult Mouse Kidney 64

6 FUTURE DIRECTIONS 71

LIST OF REFERENCES 75

BIOGRAPHICAL SKETCH 86

ABBREVIATIONS

Abbreviation	Description
α-SNAP	α-soluble NSF attachment protein
ACE	Angiotensin converting enzyme
Ang	Angiotensin II
AnnV	Annexin V
AT_1R	Type 1 angiotensin II receptor
AT_2R	Type 2 angiotensin II receptor
BrdU	Bromodeoxyuridine
CAII	carbonic anhydrase II
CD	Collecting duct
EE	Early endosome
ELISA	enzyme-linked immunosorbant assay
GAP	GTPase activating protein
GDI	GTP-dissociation inhibitor
GEP	Guanine nucleotide exchange protein
HO-1	Heme oxygenase 1
IC	Intercalated cells
L	Lysosome
LE	Late endosome
mTAL	Medullary thick ascending limb
NSF	*N*-ethylmaleimide-sensitive factor
OMCD	Outer medullary collecting duct
PI	Propidium iodide
PLP	Fixative: 2% paraformaldehyde in phosphate buffer containing lysine HCl and sodium periodate
RAS	Renin angiotensin system
RE	Recycling endosome
SNARE	soluble *N*-ethylmaleimide-sensitive fusion protein attachment protein receptor
TAL	Thick ascending limb
TGN	Trans-Golgi network
TJ	Tight junction
TUNEL	Terminal deoxynucleotidyl transferase (TdT) dUTP nick-end labeling
V-ATPase	Vacuolar proton ATPase
ZO-1	Zonula occludens 1

Abstract of Dissertation Presented to the Graduate School
of the University of Florida in Partial Fulfillment of the
Requirements for the Degree of Doctor of Philosophy

VACUOLAR H-ATPase AND THE NEPHRON: DEVELOPMENTAL APOPTOSIS AND ADULT PHYSIOLOGY

By

Lisa M. Curtis

December 2001

Chairman: Stephen L. Gluck, M.D.
Major Department: Anatomy and Cell Biology

Developmental modeling of organs and tissues occurs by cell proliferation followed by selective removal of cells by programmed cell death, or apoptosis. In the developing kidney, apoptosis begins at the tip of the papilla and progresses apically where it abruptly stops, forming the border between the outer and inner medulla. A portion of cells are removed from the immature thick limb; the remaining cells differentiate into the mature thick ascending limb in the outer medulla while the cells remaining in the inner medulla form the thin ascending limb epithelia. Intercalated cells (IC) of the collecting duct, which are characterized in part by specialized localization of the vacuolar H-ATPase (V-ATPase), are also eliminated from the inner medulla during development. The mechanisms controlling this process are not known. Studies have suggested a role for angiotensin II (Ang) in the developmental remodeling of tissues. In the first phase of this dissertation, the role of Ang in apoptosis was investigated using

developmental *in vivo* and *in vitro* models. The findings demonstrate no support for the hypothesis that Ang is involved in the regulation of apoptosis in the kidney.

A second possible mechanism for control of renal developmental apoptosis is the regulation of V-ATPase activity. The V-ATPase localizes to and functions in the acidification of various intracellular compartments and, in certain cells including the IC, is also expressed on the plasma membrane. One mechanism by which V-ATPase activity is regulated, translocation of the pump between the plasma membrane and adjacent tubulovesicles, is not well defined, but may involve the small GTP-binding proteins of the Rab subfamily.

The second phase of this dissertation was to identify candidate Rab GTPases for involvement in the trafficking of the V-ATPase. The results of the second phase demonstrate that Rabs 11, 18 and 20 colocalized with the V-ATPase, while Rab 5a and Rab 13 did not. The role of Rabs 11, 18 and 20 in V-ATPase trafficking, and the role of V-ATPase in the control of the developmental apoptotic wave in the kidney are exciting lines of future investigation.

CHAPTER 1
INTRODUCTION

Kidney Development

The urine-concentrating ability of the kidney relies in part on the salt and water gradient that exists from cortex to papilla. Functioning of this mechanism depends on the proper development of the loop of Henle and the collecting duct system; however, the regulatory controls of this developmental process are not well understood. During kidney development, the more distal region of the loop of Henle arises as an immature thick epithelium. This tissue is subsequently remodeled into the thin ascending limb, which makes an abrupt transition to the mature thick ascending limb (TAL). In contrast to the adult, in the neonatal collecting duct (CD), two types of intercalated cells (IC) are found in the inner medulla. Both α and β IC are removed from the inner medulla during the first two postnatal weeks in the rat. Such remodeling necessitates exquisite control of the sequential events of growth followed by selective removal of cells.

Apoptosis, a form of programmed cell death, is an important developmental mechanism for the sculpting of various organs, including the kidney [1, 2, 3, 4]. Previous studies have demonstrated dramatic remodeling in the neonatal rat papilla, specifically in the loop of Henle and CD [5, 6], in which apoptosis plays an essential role. In the rat papilla, Kim et al. [5] showed that a wave of apoptosis begins just proximal to the tip of the papilla in the immature thick limb epithelium and progresses to the border of the inner and outer medulla

where it abruptly stops. Those cells in this region of the nephron that survive apoptotic removal then differentiate into the ascending thin limb cells of the loop of Henle. The remaining thick epithelium differentiates into the mature TAL. In the CD, the IC are lost in different ways. The α IC, which are thought to be "acid-secreting" cells, are removed by sloughing off into the lumen and may subsequently undergo apoptosis. In contrast, the β IC, or "base-secreting" cells, are selectively removed *in situ* from the inner medullary CD by apoptosis [6]. Extensive growth also occurs during development of the renal papilla and zones of cell proliferation have been detected in the cortex and outer medulla. Little evidence of cell proliferation, however, occurs in the renal papilla [7]. The lack of cell division in the inner medulla is consistent with the thin ascending limb arising from cells of the immature thick epithelium.

The control of the balance between cell proliferation and cell death is known to be affected by the presence or absence of several growth factors such as epidermal growth factor, platelet-derived growth factor, fibroblast growth factor and transforming growth factor α and β among others [4, 8]. The process of sculpting organs during development could be regulated by gradients of these growth factors or by the presence or absence of specific growth factor receptors on the individual cells. It is also conceivable that a single growth factor may interact with two different receptors, which produce opposing actions in the cell, the balance between them determining the outcome. One such growth factor is angiotensin II. Additionally, given the different mechanism of removal of the α and β IC, and their unique distribution of the vacuolar H-ATPase (V-ATPase), the

regulation of this enzyme may influence the apoptotic process in these cells. Postnatal renal development involves establishment of acid-base regulation, including changes in the expression levels of the V-ATPase and its activity [9, 10, 11]. Changes in IC are also known to occur during this time, gradually resulting in mature expression patterns of characteristic proteins and other markers [12, 13, 14, 15]. The coincidence of changes in the functional characteristics of IC with the wave of apoptosis is intriguing and may implicate the V-ATPase in this process.

Angiotensin II

Angiotensin II (Ang) is a fragment of a precursor protein, angiotensinogen, that is produced primarily in the adult liver, but which has been identified in several organ systems of the neonatal animal including the kidney [16]. Angiotensinogen is cleaved by renin, an enzyme produced and released by cells in the juxtaglomerular apparatus of the kidney, releasing a decapeptide, angiotensin I. Angiotensin I is then further metabolized by the action of angiotensin-converting enzyme (ACE) to Ang. The components of this series of reactions make up the renin-angiotensin system (RAS) (Figure

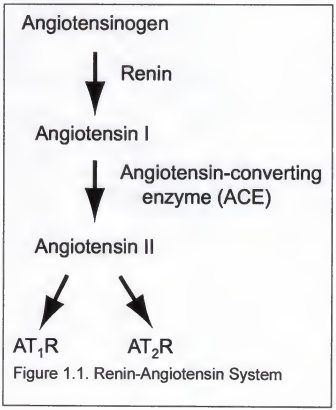

Figure 1.1. Renin-Angiotensin System

1.1). Notably, all of the components of the RAS have been identified in the neonatal rat kidney [16] and thus may act locally independently of a systemic circulation.

Two receptors for Ang have been described, the type 1 receptor (AT_1R) and the type 2 receptor (AT_2R), and evidence suggests that Ang signaling via these receptors may result in opposing effects. Many studies have suggested a proliferative effect of Ang mediated via the AT_1R in several systems including the kidney [17, 18]. Proliferation of cultured glomerular endothelial cells has been shown to respond to Ang signaling via the AT_1R [19]. Further, Ang was shown to be mitogenic for transformed TAL cells [20]. Recent studies have implicated the AT_2R as an anti-growth or pro-apoptotic receptor for Ang. Signaling via the AT_2R by Ang inhibited cell proliferation in several cultured cell types [21, 22, 23]. Apoptosis was demonstrated in Ang-treated PC12W cells, which express predominantly the AT_2R [24]. In the kidney, AT_1R protein expression has been demonstrated in several renal tubules, including the TAL and CD [25, 26, 27]. Localization of AT_1R mRNA has been identified predominantly in the cortex and outer medulla in the neonatal rat and mouse [26, 27, 28, 29]. Protein of AT_2R has been identified in the kidney in glomeruli, proximal and distal renal tubules and in vasculature [30], while AT_2R mRNA has been shown to be present mostly in the inner medulla [31].

Evidence from the disruption of the RAS either by ACE inhibition or knockouts of components of the RAS implicates this system in the development of the kidney. Angiotensinogen-knockout animals have greatly foreshortened

papillae [32, 33]. Furthermore, administration of the ACE inhibitor, enalapril, has been shown to reduce the size of the papilla, decrease the numbers of proliferating cells in the outer medulla [34] and cause abnormalities in kidney function [35]. These studies suggest that regulation of the growth of the papilla may involve the RAS. Given the identification of a local RAS and the presence of both Ang receptors in the developing kidney, Ang appears to be a good candidate for the control of the development of the loop of Henle and/or the CD. An elucidation of such a role in these developmental processes and an identification of the effects mediated by the AT_1R and AT_2R provides an important understanding of the development of the kidney. In the first phase of this dissertation, the role of Ang in apoptosis was examined using *in vivo* and *in vitro* models.

Vacuolar H-ATPase

V-ATPase in Apoptosis

Recent work has implicated the V-ATPase in cell proliferation and apoptosis. In neonatal cardiomyocytes, inhibition of V-ATPase resulted in increased expression of p53 and induction of apoptosis [36]. Neointimal myofibroblasts derived from human saphenous vein segments demonstrated increased expression of one of the subunits of the V-ATPase prior to proliferation and differentiation. Further, proliferation was reduced and apoptosis induced by V-ATPase inhibition [37]. Various cell types also exhibited sensitivity to inhibition of V-ATPase including cleavage of retinoblastoma protein, DNA fragmentation, and morphological changes consistent with apoptosis [38, 39, 36, 40, 41, 42]. Treatment of isolated neutrophils with granulocyte colony-stimulating factor

maintains expression and translocation of the V-ATPase to the membrane and prevents apoptosis in these cells [43, 44].

Structure and Function

The V-ATPase is a multisubunit enzyme involved in the acidification of intracellular compartments of cells. In certain specialized cells, V-ATPases are also located in the plasma membrane and in plasma membrane-associated compartments. The V-ATPase is composed of two separable complexes, V_1 and V_o. The V_1 complex is composed of subunits A-H that form the cytosolic head and stalk structure, which contains the ATP binding site and is the catalytic unit of the enzyme [45, 46, 47, 48]. A total of six alternating A and B subunits interact with each other in the head region. Two isoforms of the B subunit have been described, each exhibiting differing cellular distribution [49, 50, 51]. The B2 isoform appears to be more ubiquitous, while the B1 subunit has a more limited expression pattern. The E and H subunits are thought to be associated with the stalk region of the holoenzyme, while the D subunit may be positioned at the center of the A and B subunit hexagon [52, 45, 48]. The other V_1 subunits have been less well studied. The V_o complex is composed of several integral membrane proteins that form the transmembrane region of the V-ATPase and contains the channel through which the protons are released.

Regulation

Regulation of V-ATPase can be through several mechanisms. Maintenance of synthesis of V-ATPase subunits is necessary to preserve the intact enzyme and maintain the interaction between the V_1 and V_o complexes. Neutrophils grown in the absence of granulocyte colony-stimulating factor lose

expression of the 57kD B-subunit of the V-ATPase [43]. Endogenous inhibitor and activator of V-ATPase have been described. An activator of V-ATPase was identified from bovine kidney cytosol and preferentially activated plasma membrane V-ATPase in contrast to intracellular V-ATPases [53]. A low molecular weight cytosolic inhibitor of V-ATPase was also purified from bovine kidney cytosol [54]. An additional mechanism of regulation of V-ATPase activity in certain specialized cells is recruitment and polarization to specific membrane domains in response to physiological stimuli. In quiescent osteoclasts, V-ATPases are located primarily in cytosolic vacuoles. Upon activation of osteoclasts, V-ATPases are recruited to the plasma membrane to form the ruffled membrane that establishes a sealed extracellular compartment on bone [55]. Acidification of this compartment by V-ATPases is necessary for dissolution of bone hydroxyapatite, and for the activation of acid proteases involved in the degradation of bone matrix. In neutrophils, the V-ATPase is activated and becomes associated with the plasma membrane upon stimulation by phorbol myristate acetate [56].

Cell-specific, physiologically regulated polarization of V-ATPases also occurs in the kidney. In proximal tubule cells, V-ATPases are present at high densities in the brush border membrane and subapical vesicles [57]. Some experimental evidence suggests that metabolic acidosis promotes recruitment of V-ATPases from vesicles to the brush border [57]. In the CD, polarized, plasma membrane V-ATPases are found in each of the types of IC. The α IC maintains high levels of V-ATPase in the apical membrane and apical vesiculotubular

elements. The β IC contains V-ATPases in the basolateral membrane and basolateral vesicles. The localization of the V-ATPase in the mammalian kidney has been shown to be modulated by metabolic acidosis or alkalosis [57, 58]. Acidosis in the rat and rabbit was shown to alter the localization of the V-ATPase from apically located intracellular compartments to the apical plasma membrane of the α IC by immunofluorescence and immunoelectron microscopy [57, 58], although protein and mRNA expression did not appear to be changed [57]. These results suggest that the polarized vesicles containing V-ATPase were induced to relocate to and fuse with the plasma membrane in acid-loaded animals.

Rab GTPases

Although the specific signaling mechanisms involved in the relocalization of V-ATPases are not known, the Rab subclass of the small GTP-binding proteins have important roles in the recycling of many membrane proteins. The Rab subclass belongs to the larger Ras family of small GTPases, which also includes the Rac, Rho, Arf and Sar proteins [59, 60]. Although the specific function of Rab GTPases is not known, they are thought to function in vesicle trafficking and, in general, cycle between a GTP-bound, or active state, and GDP-bound, or inactive state (Figure 1.2). In the inactive state, the GDP-bound form of Rab GTPases are bound either by escort proteins in the biosynthesis pathway or by GDP dissociation inhibitors (GDI), which maintain the Rab GTPases in the cytosol, preventing their activation. The GDI along with the Rab GTPase are necessary to identify the proper target membrane to which the Rab

GTPase binds via its prenylated C-terminus (Figure 1.2, sequence A). A guanine nucleotide exchange protein (GEP) replaces the GDP with GTP thereby activating the Rab GTPase (Figure 1.2, sequence B). Active Rab GTPase recruits effector (E) molecules (Figure 1.2, sequence C), which then interact with the acceptor membrane (Figure 1.2, sequence D). Additional contacts are made between the donor vesicle and acceptor membrane through the interactions of vesicle (v)-SNAREs (**s**oluble ***N***-ethylmaleimide-sensitive fusion protein **a**ttachment protein **re**ceptor) and target (t)-SNAREs (Figure 1.2, sequence E), the former present on the donor membrane and the latter on the acceptor

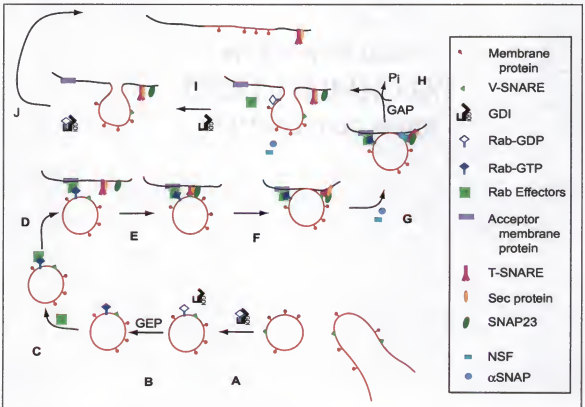

Figure 1.2. Rab GTPase cycle. The sequences of reactions involved in the translocation and fusion of vesicles from the donor membrane to the acceptor membrane are described in the text.

membrane [61]. Multiple t-SNAREs, including the SNAP-25 (**syn**aptosome-**a**ssociated **p**rotein 25) family of proteins, such as SNAP-23 in epithelia, have been shown to interact together with a v-SNARE, including those of the VAMP (**v**esicle-**a**ssociated **m**embrane **p**rotein) family. The v-SNARE/t-SNARE interactions are regulated by the Sec1 family of proteins originally described in yeast [62]. Although the specific role of Sec1 proteins is not completely clear, it has been shown that binding of the Sec1 protein to a t-SNARE of the syntaxin family prevents the interaction of syntaxin to its cognate v-SNARE [63, 64, 65]. In yeast, Sec protein may have additional or alternative roles which may be regulated by Rab GTPases [66].

The concerted interactions between the donor vesicle and the acceptor membrane by Rab GTPase effector complexes and by SNARE complexes lead to docking (Figure 1.2, sequence F). The SNARE complex is bound and disassembled by NSF (***N***-ethylmaleimide-**s**ensitive **f**actor) and α-SNAP (α-**s**oluble **N**SF **a**ttachment **p**rotein), which may also serve in the docking step (Figure 2.1, sequence G). The GTP-bound Rab GTPase undergoes hydrolysis to a GDP-bound form, facilitated by the action of a GTPase activating protein (GAP) and the donor vesicle and acceptor membranes fuse (Figure 1.2, sequence H). Rab GTPase effector molecules dissociate from the GDP-bound Rab GTPase, which is then removed from the donor membrane and retrieved by GDI (Figure 1.2, sequence I). It is not clear how the v-SNARE is recycled, however t-SNAREs of the syntaxin family are thought to be masked again by the actions of the Sec1 family of proteins (Figure 1.2, sequence J), preventing promiscuous interactions.

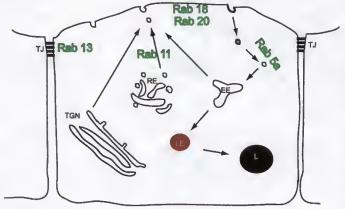

Figure 1.3. Rab GTPases in vesicle trafficking

Over 50 Rab GTPases have been identified and several have been shown to be associated with specific compartments of the cellular secretory and endocytic pathways. Certain Rab GTPases are intriguing with regard to the relocalization of the V-ATPase particularly those Rab GTPases that are critical in the endocytic or vesicle recycling pathways (Figure 1.3). Additionally, Rab GTPases that are expressed in kidney but have as yet undefined roles may also be important in the regulated trafficking of the V-ATPase. An understanding of Rab GTPase involvement in the localization of the V-ATPase provides a framework on which to examine the role of V-ATPase in apoptosis.

Rab 5a

The most well characterized Rab GTPase in the endocytic pathway is Rab 5. Three isoforms have been characterized in mammalian cells, all of which have been localized to early endocytic compartments [67] (Figure 1.3) and are important in homotypic fusion of early endosomes (EE) [67, 68, 69]. Little is known of the specific role of the b and c isoforms of Rab 5, whether they have differing or redundant roles to that of the a isoform, although different phosphorylation characteristics of the three isoforms have been described [70].

Expression of dominant negative Rab 5a constructs was shown to inhibit the fusion of EE and leads to the disruption of the early endosomal compartment [67]. Previously, Rab5a was identified in neuronal cells [71], in gastric chief cell membranes [72] and in zymogen granules of pancreatic acini [73]. The importance of Rab 5a in the endocytic pathway indicates a potential for involvement in the recycling of the V-ATPase from the plasma membrane.

Rab 11

Rab 11 has been localized to the perinuclear recycling endosome (RE) of cultured epithelial cells [74] and was shown to associate with the glucose transporter, GLUT4, which is contained in a vesicular compartment in unstimulated cells. [75]. Rab 11 is thought to be involved in the regulated recycling of proteins to the plasma membrane from RE as well as from the trans Golgi network (TGN) (Figure 1.3) [76, 77]. Rab 11a was originally cloned from rat brain and subsequently from MDCK cells and rabbit parietal cells [78, 79, 80]. A second isoform, Rab 11b, has been cloned which has significant homology to Rab 11a, although Rab 11b is coded for by a different gene than Rab 11a [81]. Localization studies do not differentiate between the two isoforms and the specific role of Rab 11b versus Rab 11a is unknown. In rabbit gastric parietal cells, Rab 11 colocalized with the H, K-ATPase and showed a change in distribution similar to that of H, K-ATPase in response to histamine [82, 83]. In activated osteoclasts, Rab 11 has been found associated with the ruffled membrane [84]. Additionally, Rab 11 was identified in esophageal epithelia [85], in uterine glandular epithelia [86], in pancreatic acini [73] and in rabbit stomach, colon, liver and kidney [87]. In uterus, Rab 11 mRNA was increased in response

to estrogen [86]. Dysplastic epithelia of the esophagus has been shown to contain elevated levels of Rab 11 [85]. The localization of Rab 11 with proteins and membrane regions that are recycled under physiological changes makes this Rab GTPase an interesting candidate to examine for a role in V-ATPase trafficking.

Rab 13

Most of the Rab GTPases, including Rab 13, have been less well studied and their roles in intracellular trafficking of vesicles have not been determined. Rab 13 was originally cloned from a Caco-2 cell line and identified in other cell lines as well as in various mouse tissues. Rab 13 was found to be associated with vesicles of fibroblasts and identified in apical membranes of epithelia [88], where it colocalized with a tight junction (TJ) protein, zonula occludens 1 (ZO-1) (Figure 1.3). These data suggest a role for this Rab GTPase in the targeting of membrane protein to the apical or basolateral membrane, or in the regulation of the tight junction [88]. Immunostaining has been demonstrated at junctional complexes in mouse small intestine, kidney, liver, heart and endothelium [88].

Rab 18

Rab 18 was cloned from mouse kidney and localized to both proximal and distal nephron segments [89]. Rab 18 immunohistochemical staining appeared more prominent at or in the apical membranes of proximal tubule cells (Figure 1.3). In contrast, in mouse intestine, Rab 18 was found in both apical and basolateral membranes. Rab 18 also has been identified in human endothelial cells [90] and, using PCR-based methodology, in human skeletal muscle [91], heart, brain, kidney, placenta, pancreas, lung and liver [90]. By Northern

analysis, Rab 18 mRNA was demonstrated in mouse kidney, liver, intestine, brain, lung, spleen and heart [90]. A role for Rab 18 has not been determined.

Rab 20

Like Rab 18, little is known of Rab 20. Originally cloned from mouse kidney, Rab 20 was detected diffusely in tubules of the mouse kidney cortex and medulla [89]. In the proximal tubule, Rab 20 was localized in apical or subapical membranes (Figure 1.3). Similarly, in mouse intestine, Rab 20 was found predominantly in the apical pole. Northern analysis has shown Rab 20 mRNA to be present in mouse kidney, liver, intestine, lung, spleen and heart, but undetectable in brain [89]. Rab 20 functions have not been described.

Although these studies demonstrate cell type and/or intracellular compartment-specific localization, the role of Rab GTPases in the movement of the V-ATPase is unknown. In the second phase of this dissertation, immunochemical and biochemical methods were employed to ascertain the expression and localization patterns of a subset of Rab GTPases in renal cell lines and in mouse kidney, and to compare their distribution with that of the V-ATPase. The results of the examination of Rab GTPases identify these small GTP-binding proteins as potential mediators of the recycling of the V-ATPase.

CHAPTER 2
MATERIALS AND METHODS

Angiotensin II Effects on Apoptosis

Animals

All animal treatments were approved by and performed in accordance with guidelines of the Institutional Animal Care and Use Committee at the University of Florida.

Developmental

After treatments, litters from pregnant rats (Harlan) were anesthetized with pentobarbital and perfused through the left ventricle with phosphate-buffered saline (10mM sodium phosphate, 150mM NaCl, pH 7.4; PBS) followed by fixative (2% paraformaldehyde in phosphate buffer containing lysine HCl and sodium periodate; PLP). Kidneys were removed, post-fixed overnight in the same fixative, washed, dehydrated and embedded in wax.

Adult

To verify the technique of TUNEL, homozygous mice carrying a targeted deletion of the heme oxygenase 1 (HO-1) gene, and their heterozygous and wild-type litter mates, were administered cisplatin (20 mg/kg at 1 mg/ml solution in sterile saline) via a single intraperitoneal (IP) injection. Three days after injection, animals were anesthetized and the tissues were processed as described above [92].

Animal Treatments

ACE inhibitor

Neonatal rat pups from 4 litters were administered enalapril (10 mg/kg bw/day), an ACE inhibitor, or the vehicle, saline, by intraperitoneal (IP) injection beginning on P1, the first day following the day of birth. Injections were continued until the day of sacrifice. On days P3 (n=2 treated, n=1 control), P6 (n=7 treated, 8 control) and P13 (n=6 treated, 5 controls), rat pups were processed for TUNEL and bromodeoxyuridine (BrdU) labeling.

Receptor blockade

Initially, postnatal day 6 (P6) neonatal rats from 2 litters were either administered Losartan (10 mg/kg/day; n=4), an AT_1R blocker, or PD123319 (10 mg/kg/day; n=4), an AT_2R blocker, or the vehicle (saline; n=4) by IP injection for a period beginning on P1 and ending on P6. Subsequently, neonatal animals from another 2 litters were administered either Losartan (20, 30, or 40 mg/kg/day; 2-3 animals/group) or PD123319 (20 or 40 mg/kg/day; 2-3 animals/group) or saline (n=3) for a period beginning on P1 and ending on P6. Rats were processed for TUNEL and BrdU labeling.

Antibodies and Reagents

Antibody to Na, K-ATPase α_1-subunit was obtained from Upstate Biotechnologies Inc (Lake Placid, NY). Antibody to bromodeoxyuridine (BrdU) was purchased from Boehringer Mannheim (Basel, Switzerland). Antibody to the type 1 receptor for angiotensin (AT_1R) was purchased from Santa Cruz Biotechnology Inc (Santa Cruz, CA). The type 2 angiotensin receptor (AT_2R) antibody was generously provided by Dr. Steven J. Fluharty (Philadelphia, PA).

Secondary antibody, rat-adsorbed, biotinylated horse anti-mouse IgG was obtained from Vector Laboratories (Burlingame, CA), as were Methyl green, the peroxidase substrates, diaminobenzidine (DAB) and Vector SG, and the avidin-biotin complex, ABC Reagent. Peroxidase-labeled goat anti-rabbit antibody and o-phenylenediamine (OPD) were purchased from Zymed (South San Francisco, CA). Terminal deoxynucleotidyl transferase (TdT) and biotinylated dUTP were purchased from Boehringer Mannheim (Basel, Switzerland). The annexin V (AnnV)/propidium iodide (PI) kit was from R&D Systems (Minneapolis, MN). Cell culture media and reagents were obtained from GIBCO BRL Life Technologies (Carlsbad, CA). For protein quantification, the BCA kit was purchased from Pierce (Rockford, IL). All other reagents were obtained from Fisher (Pittsburgh, PA) or Sigma (St. Louis, MO).

Cell Culture

Mouse outer medullary collecting duct (OMCD) cells (passages 9 to 12) and medullary thick ascending limb (mTAL) cells (passages 5 to 8) were obtained from Dr. Kirsten Madsen (University of Florida). Cells were plated on collagen-coated coverslips or chamber slides. Complete media of DMEM/F12 containing 10% NU-serum (Becton Dickenson, Bedford, MA), insulin-transferrin-selenium, 20 ng/ml hydrocortisone, and antibiotics was used for OMCD cells. Complete media, as above, additionally containing T_3 was used for mTAL cells. Media were replaced every 2-3 days until cells were 80-90% confluent. Serum starvation (serum-free) media consisted solely of DMEM/F12.

Cell Treatments

Serum starvation

Cultured cells (mTAL) were grown in complete media until confluency whereupon the complete media was replaced with serum-free media for 16 to 48 hours. Cells were subsequently washed with cold PBS, pH 7.4, fixed in 10% formalin in PBS and processed for TUNEL. No changes in TUNEL were seen in serum-starved cells relative to cells cultured in complete media (data not shown).

Angiotensin II administration

Cells (mTAL and OMCD) were grown in complete media on gelatin-coated chamber slides until confluent and serum starved for 24 hours before introduction of varying concentrations of Ang (10^{-7} to 10^{-11} M) into the media. After 16 to 24 hours of exposure to Ang, cells were washed in cold PBS, pH 7.4, fixed in 10% formalin in PBS for 10 minutes, and processed for TUNEL. For BrdU labeling, cells were exposed to Ang for 16 to 24 hours before introducing BrdU to the cultures for 2-3 hours. Cells were washed, fixed in cold acetone and processed for BrdU immunocytochemistry.

Angiotensin II receptor blockade

For TUNEL, mTAL and OMCD cells were grown in complete media to 80-90% confluence before serum starvation. Treatment of the cells with either Losartan (10^{-6} M) or PD123319 (10^{-6} M) preceded by 12 hours the introduction of varying concentrations of Ang (10^{-7} to 10^{-11} M) to the media for 24 hours. Cells were subsequently washed in cold PBS, pH 7.4 before fixation in 10% formalin in PBS. Cells were then processed for TUNEL or Ann V/PI labeling. To identify changes in proliferation, mTAL and OMCD cells were grown to confluency before

serum starvation and treatment as described above. Prior to fixation in cold acetone for 3-5 minutes, BrdU was added to the cultures for 2-3 hours. Cells were dried at room temperature and rehydrated in PBS, pH 7.4 for 15-20 minutes before being processed for BrdU immunocytochemistry.

Detection of Apoptotic Nuclei by TUNEL

Tissue sections

Wax sections of 5-6 μm were placed on gelatin-coated slides and subsequently wax was removed by immersion of the sections in decreasing concentrations of ethanol followed by dH_2O. A protocol modified from Gavrielli et al. [93] was used for TUNEL. Endogenous peroxidases were inactivated by incubation in 3% H_2O_2 and the DNA was denatured by incubation for 60 minutes in 60°C dH_2O. After preincubation in Reaction buffer (30 mM Trizma-base, pH 7.2 with 140 mM sodium cacodylate and 1 mM cobalt chloride), sections were incubated for 45 minutes at 37°C with Reaction buffer containing TdT (0.3 U/100μl) and biotinylated-dUTP (1 nmol/100 μl). Subsequently, sections were rinsed four times in Terminating buffer (300 mM NaCl, 30 mM sodium citrate). Sections were incubated with 2% BSA in phosphate buffered saline (PBS), pH 7.2 for 1 hour to block nonspecific binding and incubated with ABC Reagent for 30 minutes. After washing four times in PBS, labeling of DNA with biotinylated dUTP was developed using the peroxidase substrate, DAB. Tissues were either counterstained with Methyl Green or processed for immunolabeling of Na, K-ATPase α_1 subunit. For immunolabeling, sections were immersed in 0.1 M citrate buffer (0.1 M citric acid, 0.1 M sodium citrate, pH 6.0) in a Coplan jar, placed in a

humidified microwave, and heated on medium for 7.5 minutes to improve antigen retrieval. Cooled sections were placed in PBS before inactivation of peroxidases using 3% H_2O_2. Nonspecific binding was reduced by incubating sections with 2% BSA in PBS before incubating with antibody to the Na, K-ATPase α_1-subunit overnight at 4°C in a humidified chamber. Secondary antibody, rat adsorbed, horse anti-mouse was placed on the sections for 2 hours followed by immunodetection of Na, K-ATPase α_1-subunit using the chromagen, Vector SG. Sections were dehydrated and mounted in Permount. Sections were viewed at a magnification of 40X and random areas of at least 3-4 sections/animal were examined. The total number of apoptotic nuclei per square millimeter was calculated for each animal. Values were analyzed by unpaired t-test and ANOVA. For cisplatin-treated animals, the number of nuclei labeled in renal tubules in an average of 266 ± 55 fields were scored.

Cultured cells

Cells (OMCD or mTAL) were grown on coverslips or chamber slides. After treatments, cells were washed in sterile PBS and fixed in 10% buffered formalin. After washing in dH_2O, cells were incubated with Reaction buffer for 60 minutes at 37°C. Subsequently, cells were rinsed in Terminating buffer and processed as above for DAB. Cells were placed in PBS before inactivation of peroxidases using H_2O_2 and nonspecific binding to the sections was reduced by immersion in 2% BSA in PBS before incubating with antibody to the Na, K-ATPase α_1-subunit overnight at 4°C in a humidified chamber. Secondary antibody, rat adsorbed, horse anti-mouse was incubated on the cells for 2 hours followed by

immunodetection of Na, K-ATPase α_1-subunit using the chromagen, Vector SG. Cells were dehydrated and mounted in Permount.

Detection of Apoptotic Nuclei in Cultured Cells by Labeling of Annexin V and Propidium Iodide

Cells were grown on coverslips or chamber slides. After treatments, cells were washed in sterile PBS and incubated in 1X buffer containing AnnV (5 μg/ml) and PI (1μg/ml) for 20 minutes at 4°C. After washing in 1X buffer, cells were mounted with Crystal mount and viewed on a Zeiss fluorescence microscope. Alternatively, trypsinized and washed cells were incubated in suspension with AnnV/PI using the manufacturer's protocol.

Detection of Proliferating Cells by Immunolabeling of BrdU

Tissue sections

Wax sections of 5-6 μm were placed on gelatin-coated slides and the wax was removed by immersion in decreasing concentrations of ethanol followed by incubation in dH_2O. Sections were placed in 0.1 M citrate buffer in a Coplan jar and heated in a humidified microwave on Medium for 10 minutes to improve antigen retrieval. Cooled sections were placed in PBS before endogenous peroxidases were inactivated by incubation of the sections in 3% H_2O_2. Nonspecific binding was reduced by incubation with 2% BSA in PBS, pH 7.2 (BSA-PBS) for 1 hour. Primary antibody, anti-BrdU (1/50 dilution), was diluted in BSA-PBS and incubated on the sections overnight at 4°C. Following washing in PBS, sections were incubated in secondary antibody, rat adsorbed, biotinylated horse anti-mouse IgG (1/100 dilution in Blocking solution). Labeling of the antibody was detected using the ABC Reagent followed by DAB. After washing in

dH_2O, sections were fixed in 10% buffered formalin and washed. Antigen retrieval was improved as described above using heating in a microwave for 7.5 to 10 minutes. Removal of peroxidases was followed by blocking nonspecific binding with 2% BSA in PBS. Sections were incubated with antibody to the Na, K-ATPase α_1-subunit overnight. Subsequent to washes in PBS, sections were incubated with biotinylated secondary antibody, rat-adsorbed, horse anti-mouse, for 30-60 minutes. Immunolabeling was visualized using the chromagen, Vector SG and sections were dehydrated and mounted in Permount.

Cultured cells

Cells (mTAL or OMCD) were grown to subconfluent levels on coverslips or chamber slides. After treatments and incubation with BrdU, cells were washed three times with sterile PBS, pH 7.4 and fixed in cold acetone for 3 to 5 minutes. After removal from acetone, the coverslips or slides were dried at room temperature. Incorporation of BrdU into proliferating cells was detected using immunolabeling with an antibody to BrdU as described for tissue sections. Borders of cells were outlined by double-immunolabeling with antibody to the Na, K-ATPase α_1-subunit or to the AT_1R. Counterstaining with hematoxylin allowed for visualization of nuclei that did not incorporate BrdU.

ELISA

Nephron segments were microdissected by Dr. Jill Verlander from adult mice (C57J/6B), and processed for enzyme-linked immunosorbant assay (ELISA) in homogenization buffer (Tris-buffered saline containing 250 mM sucrose) by Ms. Wendy Wilbur. Protein content was quantified by use of the BCA kit and aliquots of the cell or tubule homogenates were then placed in microtiter

plate wells at protein concentrations of 7, 3.5, 1.75, and 0.875 mg/ml. Nonspecific binding was reduced by incubation of wells with 2% bovine serum albumin in PBS, pH 7.4 (BSA-PBS) for 1-2 hours before incubating with polyclonal antibody to the AT_2R (dilution in BSA-PBS) overnight at 4°C. Binding of secondary antibody, peroxidase-labeled goat anti-rabbit IgG, was visualized by incubation with the peroxidase substrate, OPD. The reaction was stopped with addition of H_2SO_4 and the absorbance was read at 490nm on a microtiter plate reader (BioTec) and values were plotted. Readings from wells without protein gave low background.

Rab GTPases in Mouse Kidney

Animals

Adult male, Swiss Webster mice (20-30 g; Harlan) were anesthetized with an IP dose of pentobarbital (60 mg/kg) and buffered solution was perfused through the left ventricle with or without added fixatives for all the procedures. All animal treatments were approved by and performed in accordance with guidelines of the Institutional Animal Care and Use Committee at the University of Florida.

Tissue Preparation for Immunolabeling

For immunolabeling in tissue sections, animals were perfused with phosphate-buffered saline (100 mM Na_2HPO_4, 150 mM NaCl, pH 7.4; PBS) followed by fixative. Formaldehyde at 3.7% in PBS was used for Rab 5a, 10% formaldehyde in PBS was used for Rab 11, and PLP fixative was used for Rab 13, Rab 18 and Rab 20. Two to four animals were examined for each Rab GTPase. Tissues were removed and post-fixed overnight in the same fixative

before embedding in freezing media (Rab 13) or in paraffin (all others). Sections (5 μm) were placed on gelatin-coated slides. For removal of paraffin, sections were immersed sequentially in xylenes followed by graded mixtures of ethanol and water, and rehydrated in dH_2O. Frozen sections were brought to room temperature before rehydration in PBS. Sections from paraffin-embedded, gestational rat kidneys were obtained from Dr. Stephen Gluck. Neonatal mice were fixed with 10% formalin and processed as above for paraffin embedding.

Imaging

Immunohistochemical images were obtained on a Zeiss Axiophot with a Dicomed 45 megapixel digital camera attachment (Carl Zeiss Inc, Thornwood NY). Immunofluorescent images were acquired on a Zeiss fluorescence microscope attached to a Spot digital camera (Carl Zeiss Inc, Thornwood NY). Digitized images were captured with Adobe Photoshop.

Tissue Preparation for Immunoblotting

For immunoblotting, mice were perfused with PBS, the tissues (kidney, liver, heart, intestine, brain, pancreas, stomach, spleen) were removed and the kidneys were further dissected to enrich for either cortex or medullary regions. Tissues were homogenized in Tris-buffered saline (TBS), pH 7.4 containing 250 mM sucrose and protease inhibitors (leupeptin, pepstatin and aprotinin at 1 μg/ml and polymethylsufonylfluoride (PMSF) at 0.5 mM) by two or three 10-second pulses on a Polytron while being ice cooled. Samples were then transferred to microcentrifuge tubes and centrifuged at 4°C for 10 minutes at 1000 x g. The 1000 x g supernatants were used for immunoblotting after analysis for total protein by use of the BCA Protein Assay kit.

Antibodies and Reagents

Antibody to Rab 5a (rabbit polyclonal) was obtained from Santa Cruz Biotechnology Inc (Santa Cruz, CA) along with its corresponding immunogenic peptide. Antibody to Rab 11 (mouse monoclonal) was purchased from Transduction Laboratories (Lexington, KY) and Rab 13 antibody (rabbit polyclonal) was obtained from Chemicon (Temecula, CA). Antibodies to Rab 18 and 20 (rabbit polyclonals) were a generous gift from Dr. Marino Zerial (EMBL, Heidelberg, Germany). Antibodies to the V-ATPase E-subunit (monoclonal) and to the B1 and B2 subunits (polyclonal) have been characterized previously [94, 49], as has the antibody to carbonic anhydrase II (CAII; rabbit polyclonal), which was provided by Dr. Paul Linser at the University of Florida [95, 96]. Antibody to the Na, K-ATPase α_1-subunit was purchased from Upstate Biotechnologies Inc (Lake Placid, NY). Normal horse and normal goat serum, and anti-mouse and anti-rabbit biotin-labeled secondary antibodies were purchased from Zymed (South San Francisco, CA). Peroxidase-labeled antibodies used in the immunoblotting were obtained from Amersham Pharmacia Biotech (Piscataway, NJ; anti-mouse and anti-rabbit). Fluorescent secondary antibodies were purchased from Jackson Laboratories (West Grove, PA). The Elite ABC Reagent was obtained from Vector Laboratories (Burlingame, CA). The BCA Protein Assay kit was purchased from Pierce (Rockford, IL). Cell growth media, Lipofectamine 2000 and OptiMEM were purchased from GIBCO BRL Life Technologies (Carlsbad, CA). SuperSignal West Pico chemiluminescence substrate was from Pierce (Rockford, IL). All other reagents were purchased from Sigma (St. Louis, MO) or Fisher (Pittsburgh, PA) unless otherwise indicated.

Cell Culture

MDCK cells were grown in DMEM containing 4.5 mM glucose, 1% nonessential amino acids, and 10% fetal bovine serum. Media was changed every 2–3 days and cells were passaged approximately every 5 days at confluency. LLC-PK_1 cells were cultured in Media 199 containing 10% fetal bovine serum (FBS). OMCD cells were cultured as described previously.

Immunostaining of Mouse Kidney

Enzyme immunostaining

Hydrated sections were washed in PBS with or without antigen retrieval (see Table 2.1) and endogenous peroxidase activity was removed with 3% H_2O_2 in dH_2O. Sections were incubated with blocking solution for 1-2 hours to block nonspecific binding, followed by incubation with primary antibody in blocking solution overnight in a humidified chamber at 4°C. As a negative control in some experiments, primary antibody was incubated with the corresponding immunizing peptide prior to incubation on the sections overnight (Table 2.1). Additional

Table 2.1. Conditions of enzyme immunolabeling of mouse tissue (ND=not done; NHS=normal horse serum; NGS=normal goat serum; SDS=sodium dodecyl sulfate)

Rab	Antigen Retrieval	Blocking solution	Primary antibody	Biotin-labeled Secondary antibody	Peptide	Subsequent labeling
5a	ND	10% NGS in PBS	2 μg/ml	Goat anti-Rabbit, 1/100	10 μg/ml	Co-labeled with V-ATPase E subunit
11	1% SDS in PBS	10% NHS in PBS	10 μg/ml	Goat anti-Mouse IgG, 1/100	ND	Co-labeled with CAII

negative controls were sections incubated with mouse (Rab 11) or rabbit (Rab 5a) IgG. Sections were then washed with PBS, incubated with biotin-labeled secondary antibody for 1 hour at room temperature, washed, and incubated with Elite ABC Reagent. After washing with PBS, immunoreactivity was visualized with DAB. The peroxidase activity of the secondary antibody was eliminated by reincubation in H_2O_2 as above. The Rab 5a sections were incubated with blocking solution containing 20% fetal calf serum, 1% polyethylene glycol in PBS, and then with a ½ dilution of E subunit culture supernatant in the blocking solution. The Rab 11 sections were incubated again in 10% NHS-PBS, and then with antibody to CAII (1/400-1/800 dilution in NHS-PBS) to facilitate identification of tubules. Sections were washed and incubated with Elite ABC Reagent, and E subunit labeling or CAII labeling was visualized with the Vector SG chromagen substrate. Mounted sections were examined by light microscopy.

Fluorescence immunohistochemistry

Hydrated sections were treated for antigen retrieval or to reduce autofluorescence (see Table 2.2) before being incubated with blocking solution for 1-2 hours followed by incubation with primary antibody diluted in blocking solution for 2 hours in a humidified chamber at room temperature. Negative controls included sections incubated without antibody, or with rabbit and mouse IgG instead of specific antibodies. Additionally, peptide competition was used for Rab 18 and Rab 20 antibodies. Subsequently, sections were washed and incubated with the secondary antibodies, fluorescein-labeled anti-rabbit IgG or Texas Red-labeled anti-mouse IgG, for 15 minutes at room temperature. Sections were washed and mounted before observation. Simultaneous double

labeling for V-ATPase E subunit (1/3 dilution) with Rab 18 or Rab 20 was used to identify IC. For Rab 13, subsequent labeling with V-ATPase E subunit (1/3 dilution) or Na, K-ATPase α_1 subunit (1/1000 dilution) in blocking solution was used to differentiate the tubules in the outer medulla (OM). A 1-2 hour primary and 1 hour secondary antibody incubation were used for the subsequent labeling.

Table 2.2. Conditions of fluorescence immunolabeling of mouse tissue (ND=not done; NHS=normal horse serum; BSA=bovine serum albumin; RT=room temperature)

Rab	Embed	Pretreat	Antigen Retrieval	Blocking solution	Washing buffer	Primary antibody	Peptide
13	Frozen	ND	0.01% saponin in 0.02% BSA-PBS; 30 min @ RT	0.02% BSA-PBS	0.02% BSA-PBS	1/500 or 1/1000	ND
18	Paraffin	50mM NH_4Cl 15 min @ RT	ND	10% NHS-PBS	PBS	1/10 dilution	20μg/ml
20	paraffin	50mM NH_4Cl 15 min @ RT	ND	10% NHS-PBS	PBS	1/8 dilution	20μg/ml

Detection of Rab GTPases in Mouse Tissues

SDS-PAGE

SDS-PAGE was performed using the Mini-Protean II blotting system (BioRad) at 100-200V for 60-105 minutes. Samples of 30 μg total protein/lane were heated (65°C or boiled) for 5 min in sample buffer containing

βmercaptoethanol (β-ME; BioRad) and separated by SDS-PAGE with a 4% polyacrylamide stacking gel and a 12% running gel. Samples evaluated for Rab 11 were placed in sample buffer without β-ME to avoid overlapping of the band for Rab 11 (23 kD) with that of the mouse IgG light chain present in the mouse tissues, and were separated in gels without added SDS. Under these conditions, the IgG heavy and light chains remained as heterodimers, enabling separation from the Rab 11 polypeptide (data not shown). A duplicate gel analyzed by immunoblotting using only peroxidase-labeled anti-mouse IgG to detect the endogenous mouse IgG confirmed the results.

Immunoblotting

Immunoblotting was performed using standard techniques. Proteins were transferred to membranes in a wet transfer at 100V for 1 hour using the Mini Trans-blot apparatus (BioRad) immersed in ice. Consistent protein loading across lanes was verified by Ponceau S staining of the membranes before proceeding with the immunoblotting. For Rab 5a, 11, 13, and 20, membranes were incubated in Tris-buffered saline (10mM Tris-HCl, 100mM NaCl, pH 7.4) containing 5% milk and 0.1% Tween 20 (TBST-milk) to block nonspecific binding. Membranes used for Rab 18 were incubated with TBS containing 5% ovalbumin and 0.1% Tween 20. The same solution used to block nonspecific sites on membranes was used for dilution of the corresponding antibodies. Antibody to Rab 5a was used at a dilution of 1:200. Rab 18 and Rab 20 antibodies were diluted 1/200 or 1/500, Rab 11 antibody was diluted at 1:1000, and Rab 13 antibody at 1:2000. Primary antibodies were incubated with the membrane overnight at 4°C. In order to establish specificity of binding, in some

experiments, primary antibodies were preincubated with their corresponding peptides or polypeptide before incubation on the membrane. Immunizing peptide for Rab 5a (10 μg/ml), Rab 18 (5 μg/ml) and Rab 20 (5 μg/ml), and recombinant Rab 11 polypeptide (see below; 0.1 μg/ml) were used. No immunogen was available for Rab 13. Peroxidase-labeled secondary antibodies, anti-mouse (1/5000 dilution) for Rab 11, anti-rabbit (1/5000 dilution) for Rab 5a, 13, 18, and 20, were incubated for 1 hour at room temperature. Labeling was detected using the SuperSignal West Pico Chemiluminescence substrate. Bands were imaged and quantified using the Alpha Innotech system (BioRad, Hercules CA). Tissue blots were done at least 2 times for each Rab GTPase.

Generation of recombinant Rab 11 immunogen

Primers containing restriction sites for BamH1 and EcoR1 were obtained from Operon Technologies (Alameda CA) for polymerase chain reaction (PCR) amplification of the segment of the human Rab 11 cDNA encoding the immunogenic polypeptide, amino acid residues 86-207 (5'-CCCGGATCCGGTGCCTTATTGGTTTA-3'; 5'-CCCGAATTCCTTGTTTTCAGT-GGTTG-3'). PCR was performed using Taq polymerase and a human kidney cDNA library (Clontech). Optimized PCR conditions were 94°C, 3 minutes; 35 cycles of 94°C, 1 minute, 58°C, 1.5 minutes, 72°C, 2 minutes; followed by a final extension at 72°C, 2 minutes. The 384 base pair amplified fragment was treated with BamH1 and EcoR1 restriction enzymes simultaneously and ligated into the same restriction sites of the pGEX-2TK vector (Invitrogen). Competent E. coli (Max efficiency cells, GIBCO Life Technologies) were transformed with the

construct using standard procedures [97]. Following induction with IPTG (0.1mM) for 3 hours at 37°C, the human Rab 11 fragment–GST fusion protein was purified using glutathione-agarose beads [97]. Protein was measured as absorption at 280 nm wavelength.

Isolation of Mouse Kidney Fractions by Differential Centrifugation

Mice were perfused with PBS containing 2 mM EDTA (PBS-E). Both kidneys were removed and a medulla-enriched portion was dissected free. Samples from 1-2 mice were placed in 1.5 ml PBS-E containing protease inhibitors (leupeptin, pepstatin and aprotinin at 1 μg/ml and PMSF at 0.5 mM; PBS-E*) and homogenized on ice using two or three 10-second pulses of a Polytron while immersed in ice. The samples were transferred to microcentrifuge tubes and centrifuged at 1000 x g (1K) for 10 minutes at 4°C. The supernatant was subjected to sequential centrifugation at 3000 (3K), 8000 (8K), and 15000 x g (15K) for 10 minutes at each step, and finally at 100,000 x g (100K) for 1 hour. Aliquots of supernatants from each step of the differential centrifugation were taken for immunoblotting. The pellets from each step of the differential centrifugation were washed in 120 μl PBS-E* before resuspension in 100μl (3K, 8K, 15K) or 200 μl (100K) PBS-E*. Aliquots of each of the pellets and the supernatants were taken for protein analysis using the BCA Protein Assay kit. SDS-PAGE and immunoblotting on the Rab GTPases in the differential centrifugation fractions was performed as described above. Likewise immunoblotting for CAII and the V-ATPase subunits A, B1, B2 and E were performed as above. For Na, K-ATPase α_1-subunit labeling, a 7.5% running gel

was used and 5 μg total protein/lane was applied. For Na, K-ATPase α_1-subunit, CAII labeling and labeling of the V-ATPase subunits, membranes were incubated in TBST-milk and incubated as described above. Antibodies to the Na, K-ATPase α_1-subunit or to CAII were used at 1/10,000 dilution; sera containing antibodies to the A, B1 or B2 subunit of V-ATPase were diluted at 1/200. The anti-E subunit culture supernatant was diluted 1/5. Each Rab GTPase was examined using blots from at least two experiments.

Characterization of Mouse Kidney Fractions on Percoll Gradients

The 15K or 100K membranes from the differential centrifugation were subjected to self-generated Percoll gradients. Percoll was made isotonic by the addition of 1.5 M NaCl to a final concentration of 0.15 M NaCl before further dilution with PBS-E to the starting density of the Percoll solution (1.02828 g/ml; 18% Percoll). Vesicles were expected to be at densities between 1.01 and 1.04 g/ml. The conditions for optimal separation of 1.018 g/ml and 1.033 g/ml density marker beads were therefore initially established by testing different centrifugation times and Percoll densities on density marker beads (Figure 2.1). Membrane samples were brought to 200 μl with PBS-E*, if necessary, and mixed with the Percoll solution before centrifugation at 20,000 g for 15 minutes in a Ti70.1 rotor (Beckman). Nine fractions were collected by a blunted 27-gauge needle attached to an insulin syringe beginning at the top of the 7 ml gradient and continuing to the bottom of the tube. Density marker beads run in parallel in an identical tube indicated that fractions #1 and #2 were taken at the levels of marker beads corresponding to a density of 1.018; fractions #7 and #8 corresponded to 1.033 g/ml; and fraction #9 corresponded to densities of 1.049-

1.121 g/ml. The collected fractions were diluted at least 4-fold with PBS-E*. The fractions from the 15K membranes were centrifuged at 15,000 x g for 15 minutes with or without a preliminary 100,000 x g spin to remove Percoll. Fractions from 100K membranes were centrifuged twice at 100,000 x g for 60 minutes. Percoll fraction pellets were resuspended in sample buffer containing β-ME and stored at -70°C until evaluated by immunoblotting as described above.

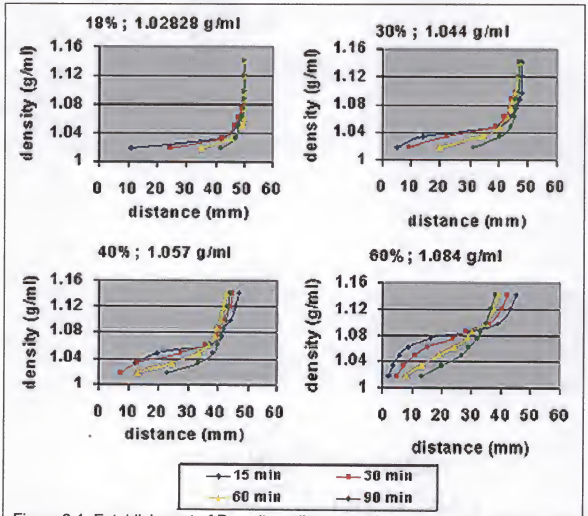

Figure 2.1. Establishment of Percoll gradient conditions. Density marker beads were centrifuged at 20,000 x g in differing Percoll densities for 15, 30, 60 or 90 minutes. The position of each of the marker beads was plotted as distance from the top of the gradient versus the density of each of the marker beads.

CHAPTER 3
ANGIOTENSIN II EFFECTS ON APOPTOSIS

In vivo Studies

Establishment of Cell Proliferation and Cell Death Techniques

Cell proliferation

Cell proliferation was detected in tissue sections and in cell culture by immunolabeling of bromodeoxyuridine (BrdU), a thymidine analog that incorporates into replicating DNA. Labeling of BrdU in proliferating cells (Figure 3.1) in a wax section of neonatal (postnatal day 6, P6) rat can clearly be seen in the nephrogenic zone and in the medullary rays. No evidence of proliferation was observed in the medulla. Prominent double-labeling of α_1-subunit of Na, K-ATPase identified distal tubules. Lower intensity labeling of Na, K-ATPase α_1-subunit was seen in collecting duct. No proliferating cells were noted in other regions of the nephron.

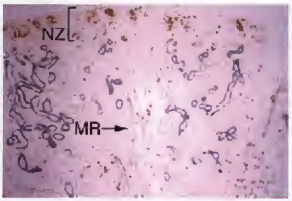

Figure 3.1 Representative BrdU labeling in mouse kidney section (NZ= nephrogenic zone; MR=medullary ray).

Cell death

Cell death was detected by terminal deoxynucleotidyl transferase (TdT)-mediated nick end labeling (TUNEL) on wax sections and in cell cultures. Apoptotic nuclei are indicated by the arrows in the micrograph of a wax section

treated with the TdT enzyme and biotin-labeled dUTP (Figure 3.2, panel 1). Low background was seen in negative control sections (data not shown). As a positive control, sections were treated with DNase I prior to incubation in the TUNEL reaction (Figure 3.2, panel 2). All nuclei appeared to display labeling by TUNEL in the positive control sections. Similarly, TUNEL in cultured mTAL cells were clearly identifiable (Figure 3.2, panel 3). DNase I-treated cells were extensively labeled by TUNEL (Figure 3.2, panel 4).

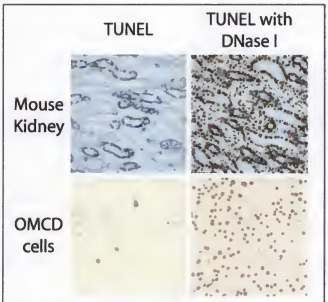

Figure 3.2 Specific labeling by TUNEL.

In order to verify the specificity of the TUNEL technique, a renal injury model, was examined. Cisplatin, an anticancer drug, induces necrosis at high doses, however, lower doses produce both apoptosis and necrosis. Transgenic mice deficient in the stress protein heme oxygenase 1 (HO-1), and their wild type littermates, were given low dose cisplatin or the vehicle saline [92]. Cisplatin-treated mice exhibited apoptosis in proximal and distal nephron as well as some evidence of necrosis. Saline-treated animals showed little or no injury. Homozygous mice deficient in HO-1 showed greater injury than their wild type littermates. Labeling was seen only in apoptotic nuclei and not in necrotic nuclei nor in cellular debris, confirming the specificity of the conditions used.

Treatment of neonatal rat pups with an ACE inhibitor

Kidneys from neonatal animals administered the ACE inhibitor, enalapril, exhibited no changes in the labeling of apoptotic cells by TUNEL at any of the

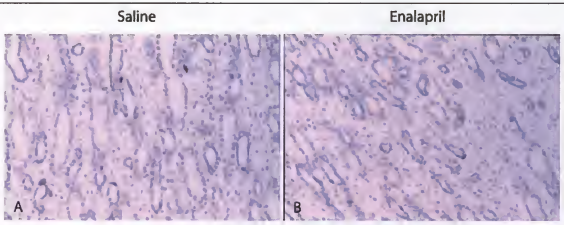

Figure 3.3 Representative photomicrographs of TUNEL labeling in kidney sections from postnatal day 6 rats treated with either the vehicle saline or the ACE inhibitor, enalapril.

time points examined (postnatal day (P) 3, 6 or 13) in the developing loop of Henle or CD (Figure 3.3). Additionally, no gross morphological changes were observed in the papilla of these neonates. The lack of changes in these animals may be due to the low dosage of ACE inhibitor used. Additionally, enalapril is inactive unless converted to enalaprilat by enzymes in the liver. Since at birth, rats do not have fully developed liver function, the enalapril given to the newborn rats may not have been successfully converted to the active form in this time period.

Treatment of neonatal rat pups with an AT_1R or AT_2R blocker

To examine the RAS at the level of Ang signaling, neonatal rats were treated with differing concentrations of the AT_1R blocker, Losartan, or the AT_2R

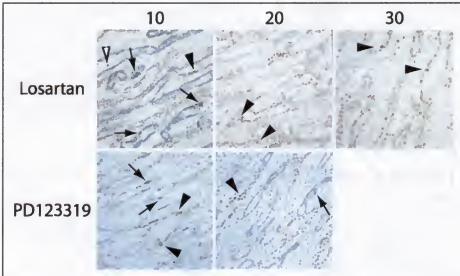

Figure 3.4. TUNEL in neonatal kidneys of P6 rats treated with Losartan or PD 123319. Arrows indicate apoptotic cells in TAL. Solid arrowheads indicate apoptotic cells in CD. Open arrowhead points to apoptotic cell in the lumen.

blocker, PD123319. In kidney sections, no differences in apoptosis in either the thick epithelium of the loop of Henle or in cells of the CD were seen. Representative micrographs of TUNEL in kidney sections of animals treated with

Table 3.1 Apoptotic indices of neonatal rat pups treated with Losartan, PD123319 or saline (ND=not done; SE=standard error)

Daily dose	Saline	Losartan	PD123319
10 mg/kg/bw	4.37 1.32	2.1 3.88 1.77	3.82 4.82 3.16
Mean ± SE	2.85 ± 1.53	2.58 ± 0.65	3.93 ± 0.48
20 mg/kg/bw	4.21 4.51 2.26	2.68 0.37	5.98 3.64
Mean ± SE		1.525 ± 1.16	4.81 ± 1.17
30 mg/kg/bw		5.86 0.16	ND
Mean ± SE		3.01 ± 2.85	
40 mg/kg/bw		4.77 0.53	4.14 2.95
Mean ± SE	3.66 ± 0.71	2.65 ± 2.12	3.55 ± 0.60

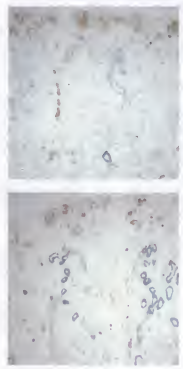

Figure 3.5 BrdU labeling in neonatal kidneys of P6 rats treated with Losartan or PD123319.

a daily dose of 10, 20 or 30 mg/kg/bw Losartan or with 10 or 20 mg/kg/bw PD123319 are shown in Figure 3.4. Apoptotic indices for the treated animals and the Group means are given in Table 3.1. Additional wax sections processed for BrdU labeling followed by double-labeling with the α_1-subunit of Na, K-ATPase for tubule identification also showed no significant differences between the saline treated animals and those treated with Ang receptor blockers. Representative photomicrographs of BrdU labeling in kidney sections of animals treated with 20 mg/kg bw/day dosages are shown in Figure 3.5.

In vitro Studies

Localization of the AT_1R in cultured cells by immunocytochemistry and AT_2R in microdissected tubules by ELISA

Acetone-fixed OMCD cells grown to confluency in serum-containing media demonstrated immunolocalization of the AT_1R predominantly in intracellular compartments in these cells (Figure 3.6). Similar results were seen in mTAL cells. Using ELISA, AT_2R was identified in mouse nephron segments (Figure

3.7). Optical density data were plotted against protein concentrations. Highest levels were seen in TAL and distal convoluted tubule with lower levels in proximal tubule and glomerulus. Wells containing protein but without primary antibody demonstrated only background binding.

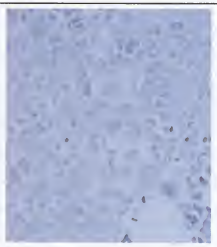

Figure 3.6 AT_1R labeling in OMCD cells.

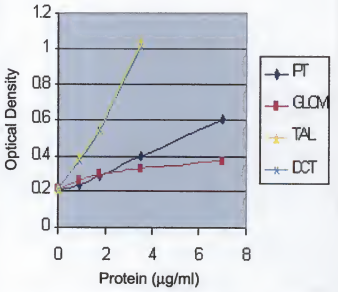

Figure 3.7 ELISA analysis of AT2R in nephron segments. (PT=proximal tubule; GLOM=glomerulus; TAL=thick ascending limb; DCT=distal convoluted tubule)

Evaluation of the response of mTAL and OMCD cells to treatment with Ang

Cells (mTAL and OMCD) treated with varying concentrations of Ang demonstrated no qualitative changes in TUNEL between the different concentrations of Ang relative to those that remained in serum-free media without Ang. Also, no differences in the numbers of cells stained for BrdU incorporation could be identified. Representative photomicrographs of BrdU labeling in mTAL cells treated with 0, 10^{-7}, 10^{-8}, 10^{-9}, 10^{-10} and 10^{-11} M Ang are shown in Figure 3.8. Similar results were seen with OMCD cells.

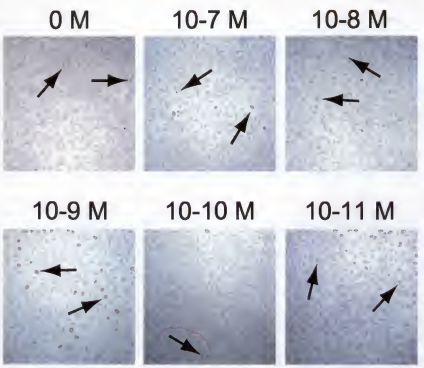

Figure 3.8 BrdU labeling of mTAL cells treated with varying concentrations of Ang.

Effects in mTAL and OMCD cells treated with Ang with and without blockade of either the AT_1R or the AT_2R

Treatment of mTAL and OMCD cells with either the AT_1R or AT_2R blocker in the presence of Ang did not alter the level of apoptotic cells as identified by either TUNEL or Ann V/PI labeling. The differing concentrations of Ang treatment relative to the control cells (no Ang present) did not have any difference in labeling. Regardless of the timing of labeling with Ann V and PI, most cells remained unstained, indicating healthy cells. Some cells were stained with both Ann V and PI, indicating necrotic cells, while very few cells were positive only for Ann V (apoptotic cells) in any of the samples (data not shown). Treatments with the Ang receptor blockers did not appear to alter the numbers of BrdU-positive cells either regardless of Ang concentration used in the presence or absence of

receptor blockers. Representative photomicrographs of BrdU labeling of cells are shown in Figure 3.9.

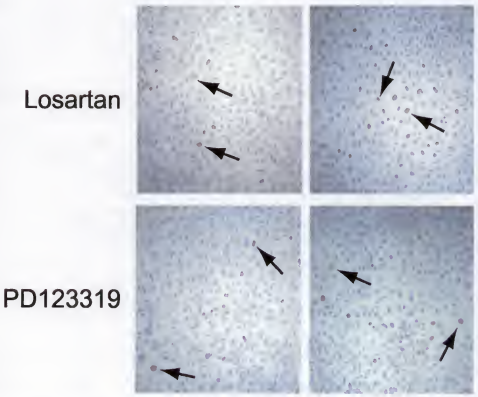

Figure 3.9 BrdU labeling of mTAL cells treated with Losartan or PD123319 in the presence or absence of Ang.

CHAPTER 4
RAB GTPases AND V-ATPase IN ADULT MOUSE KIDNEY

Tissue- and cell-type specific distribution of Rab GTPases in the mouse kidney

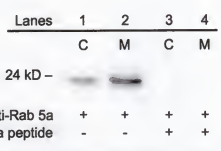

Figure 4.1. Representative blots of reactivity of Rab 5a antibody. Kidney cortex (C) and medulla (M) were blotted with anti-Rab 5a in the absence (lanes 1 and 2) or presence of immunizing peptide (lanes 3 and 4). A 24 kD band was found that was not seen when Rab 5a was incubated on the blot in the presence of peptide.

Rab 5a

A specific Rab 5a immunoreactive polypeptide was identified in mouse kidney. Mouse kidney cortex and medulla incubated with anti-Rab 5a demonstrated a single band at 24 kD (Figure 4.1, lanes 1 and 2). A similar blot incubated with anti-Rab 5a in the presence of the Rab 5a immunizing peptide had no immunoreactive bands (Figure 4.1, lanes 3 and 4). Immunoblots of various mouse tissues demonstrated ubiquitous

Figure 4.2. Rab 5a immunoreactivity in mouse tissues. Mouse tissues (30 μg total protein) were homogenized and processed for immunoblotting, run on SDS-PAGE and immunoblotted with anti-Rab 5a. C=kidney cortex, M=kidney medulla, B=brain, L=liver, St=stomach, I=small intestine, H=heart, P=pancreas, S=spleen.

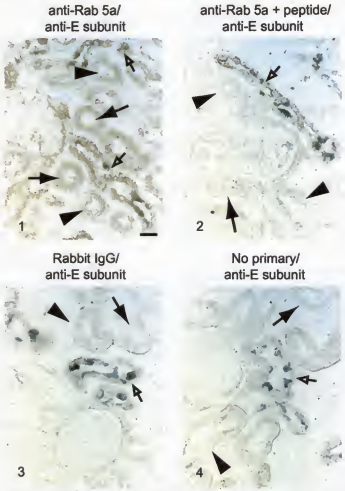

Figure 4.3. Representative images of Rab 5a immunoreactivity in mouse kidney cortex. (1) Immunostaining for Rab 5a (DAB; brown) is present as diffuse cytoplasmic staining in epithelial cells of proximal (solid arrowheads) and distal (solid arrow) tubules and CD (open arrows). Double labeling for V-ATPase (Vector SG; blue) identified IC of CD. (2) Preincubation of Rab 5a antibody with immunizing peptide before incubation on sections removed most of the Rab 5a labeling. Double labeling with E subunit antibody identified IC. (3) Immunostaining with Rabbit IgG instead of anti-Rab 5a demonstrated background staining. (4) Incubation of sections with only blocking solution instead of anti-Rab 5a showed background labeling. Labeling of E subunit identified IC.

expression of Rab 5a. In all tissues (Figure 4.2), a major immunoreactive polypeptide was observed at 24 kD. Highest expression was observed in brain with moderate levels evident in kidney cortex and medulla, stomach, heart, pancreas and spleen. Lower level expression was seen in liver, whereas no significant expression was detected in small intestine.

In adult mouse kidney sections (Figure 4.3), Rab 5a immunostaining was localized to epithelial cells of proximal and distal nephron as well as collecting duct in a diffuse

staining pattern (Figure 4.3, panel 1). Double labeling for E subunit was seen in IC of CD. The Rab 5a staining was largely removed by preincubation of the antibody with the immunizing peptide (Figure 4.3, panel 2). Similar minimal background staining was observed in sections incubated with rabbit IgG (Figure 4.3, panel 3) or no primary antibody (Figure 4.3, panel 4) instead of the specific Rab 5a antibody.

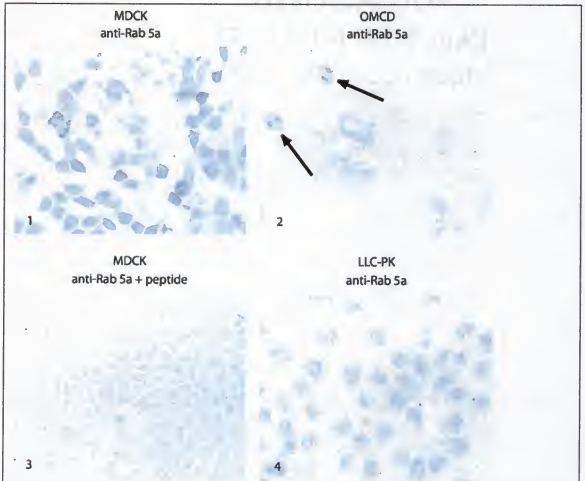

Figure 4.4. Rab 5a immunoreactivity in cultured cells. Cultured cells grown on coverslips were fixed and processed for enzyme immunocytochemistry using an antibody to Rab 5a. (1) MDCK cells, (2) OMCD cells, arrows indicate mitotic figures, (3) antibody competition in MDCK cells and (4) LLC-PK cells

Immunocytochemical labeling of Rab 5a in MDCK (Figure 4.4, panel 1), LLC-PK (Figure 4.4, panel 4) and OMCD (Figure 4.4, panel 2) cells showed a diffuse pattern of expression in interphase cells. Rab 5a was seen to associate with mitotic figures in dividing OMCD cells (arrows, Figure 4.4, panel 2). Preincubation of the specific antibody with the immunizing peptide prior to incubation on MDCK cells resulted in no labeling (Figure 4.4, panel 3). Similar results were seen in LLC-PK and OMCD cells (data not shown).

Rab 11

A specific Rab 11 immunoreactive 23 kD polypeptide was observed in mouse tissues. Competition experiments (Figure 4.5) using recombinant Rab 11 polypeptide demonstrated specificity of the immunoreactivity. Blots of kidney cortex and medulla incubated with anti-Rab 11 (Figure 4.5, lanes 1 and 2) contained one reactive band that was removed on blots incubated with anti-Rab 11 in the presence of recombinant Rab 11 polypeptide (Figure 4.5, lanes 3 and 4). Immunoblots of Rab 11 in mouse tissues (Figure 4.6) showed high expression in kidney cortex and

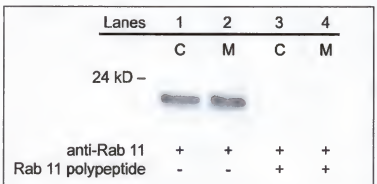

Figure 4.5. Immunoblotting with antibody to Rab 11. Homogenized kidney cortex (C) or medulla (M) tissue immunoblotted with anti-Rab 11 (lanes 1 and 2) or with anti-Rab 11 in the presence of the immunogenic polypeptide (lanes 3 and 4). A 23 kD band was present in both kidney regions that was eliminated when the blot was incubated with anti-Rab 11 in the presence of polypeptide.

medulla, brain, and stomach with lower levels of reactivity in liver, heart, pancreas and spleen. No immunoreactive bands were seen in small intestine.

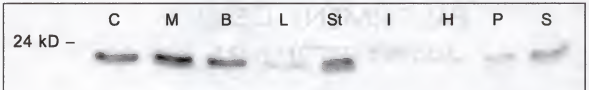

Figure 4.6. Representative immunoblot of mouse tissues with antibody to Rab 11. Mouse tissues were homogenized and processed for immunoblotting as described in Figure 4.2 and in Materials and Methods with antibody to Rab 11.

In mouse kidney sections (Figure 4.7), Rab 11 immunostaining was abundant in distal convoluted tubule cells (panel 1), connecting segment and cortical CD (panels 1, 2 and 4). Colocalization studies with antibody to CAII, which strongly stains IC [96], showed that the Rab 11 immunostaining of the CD is predominantly at the apical borders of principal cells rather than in IC (Figure 4.7, panels 3 and 4). Occasionally, immunostaining of Rab 11 was seen in the apical brush border of proximal tubule cells (Figure 4.7, panel 2). Sections incubated with mouse and rabbit IgG (Figure 4.7, panel 5) or no primary antibody (Figure 4.7, panel 6) demonstrated only nonspecific staining of interstitium.

Neonatal rats immunolabeled for Rab 11 (Figure 4.8) demonstrated staining in apical regions of epithelial cells of certain tubules in the developing cortex. Amplified expression of Rab 11 is seen in apical regions of individual cells in certain tubules. The identity of the differing tubules was not ascertained.

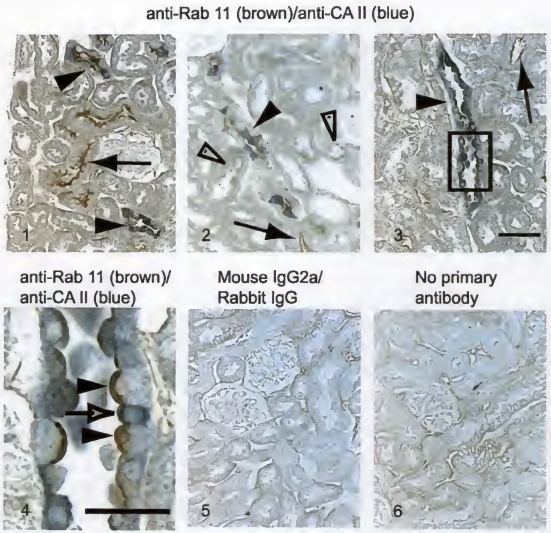

Figure 4.7. Images of Rab 11 immunolabeling of mouse kidney. (1), (2) and (3). Labeling with Rab 11 (brown) and CAII (blue) in cortex. Labeling of Rab 11 and CAII in CD or connecting tubule (closed arrowhead), in distal convoluted tubule (closed arrow), and in proximal tubule (open arrowhead). Box in panel 3 is enlarged in panel 4. Magnification bar is 100 μm and is indicative of magnification of all panels except 4. (4) Labeling in CD of Rab 11 in apical membrane of principal cells (brown, closed arrowheads) and of CAII in cytoplasm of IC (blue, open arrow). Magnification bar is 50 μm. (5) Negative control section incubated with Mouse IgG2a and Rabbit IgG instead of specific antibodies. (6) Negative control section incubated without primary antibody.

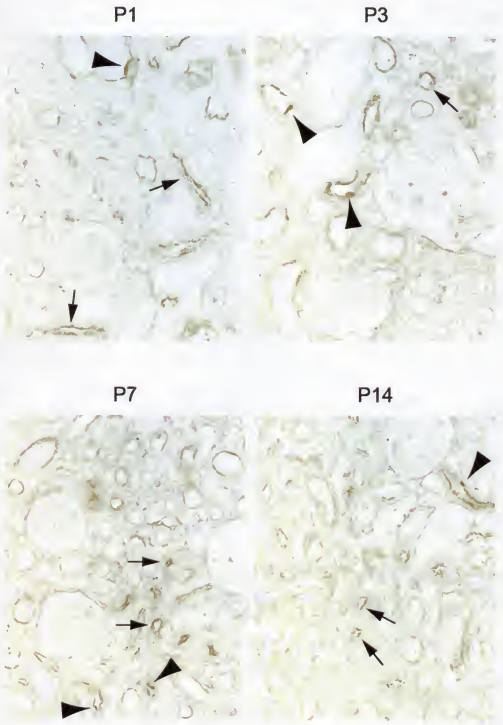

Figure 4.8. Representative images of neonatal expression of Rab 11 in mouse kidney. Mouse kidney sections from postnatal day 1 (P1), P3, P7 and P14 demonstrate apical labeling of epithelial cells (solid arrows). Certain cells (solid arrowheads) demonstrate accentuated apical labeling for Rab 11.

Rab 13

An anti-Rab 13 immunoreactive 25 kD polypeptide was found in kidney

Figure 4.9. Representative immunoblot of mouse tissues with anti-Rab 13. Mouse tissues were homogenized and processed for immunoblotting as described in Figure 4.2 and in Materials and Methods with antibody to Rab 13.

cortex and medulla, brain and heart (Figure 4.9), with lower levels of reactivity in stomach. Little or no reactivity was seen in liver, small intestine, pancreas or spleen. Additional higher molecular weight immunoreactive polypeptides were observed in brain, stomach and heart, with highest immunoreactivity to a polypeptide in brain. The identity of the additional immunoreactive species is unknown. The immunogen was not available for peptide competition.

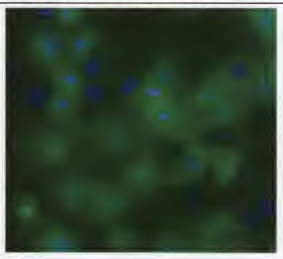

Figure 4.10. Immunolabeling of endogenous Rab 13 in MDCK cells.

Endogenous Rab 13 localization in MDCK cells appeared to be mostly perinuclear with some diffuse staining in cytoplasm (Figure 4.10). No membrane staining was observed.

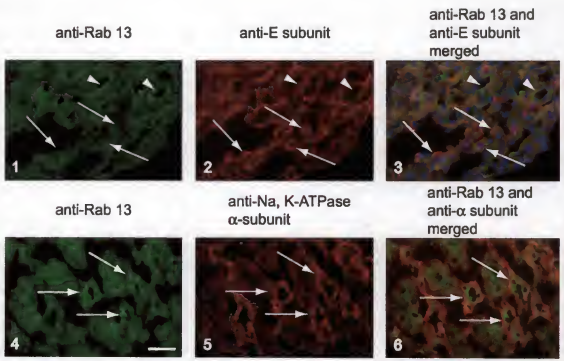

Figure 4.11. Pattern of expression of Rab 13 in mouse kidney outer medulla. (1) Fluorescence image of mouse kidney section immunolabeled with anti-Rab 13. Arrowheads indicate apical staining in thick ascending limb. Arrows point to intercalated cells which are not labeled. (2) The same section as in 1 demonstrating immunolabeling with anti-E subunit of the V-ATPase. Arrows and arrowheads are as in 1. (3) Merged image of 1 and 2 demonstrating separate localization of Rab 13 and V-ATPase E subunit. (4) Fluorescence image of mouse kidney section immunolabeled as in 1. Arrows point to apical labeling of Rab 13 in thick ascending limb. Bar is equal to 100 μm and is indicative for all panels. (5) The same section as in 4 demonstrating immunolabeling with anti-Na, K-ATPase α1-subunit. Arrows point to thick ascending limb. (6) Merged image of 4 and 5 demonstrating co-localization of Rab 13 and Na, K-ATPase α1-subunit in thick ascending limb.

In the mouse kidney, Rab 13 immunostaining (Figure 4.11, panels 2, 3, 5 and 6) was seen in the apical cytoplasm of TAL cells of the outer medulla. The identification of TAL cells was confirmed by dual labeling with either antibody to the E-subunit of V-ATPase (Figure 4.11, panel 2), which labels IC of the CD, or antibody to Na, K-ATPase α_1-subunit (Figure 4.11, panel 5), which strongly

labels basolateral membranes of the TAL and only moderately labels CD basolateral membranes. Merged images of the Rab 13 and E subunit staining (Figure 4.11, panel 3) show no colocalization to the same tubules, however, merged images of the Rab 13 and Na, K-ATPase staining (Figure 4.11, panel 6) verify localization of Rab 13 immunostaining with Na, K-ATPase in TAL cells.

Rab 18

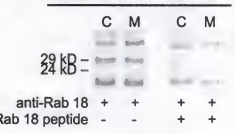

Figure 4.12. Immunoblotting with antibody to Rab 18. Homogenized kidney cortex (C) or medulla (M) tissue immunoblotted with anti-Rab 18 (lanes 1 and 2) or with anti-Rab 18 in the presence of the immunogenic peptide (lanes 3 and 4).

Antibody to Rab 18 specifically recognized a 29 kD band (Figure 4.12, lanes 1 and 2). Labeling of this band in kidney cortex and medulla was eliminated in the presence of the Rab 18 immunizing peptide (Figure 4.12, lanes 3 and 4), suggesting specificity of the

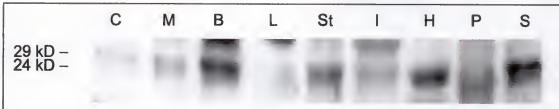

Figure 4.13. Representative immunoblot of mouse tissues with antibody to Rab 18. Mouse tissues were homogenized and processed for immunoblotting as described in Figure 4.2 and in Materials and Methods with antibody to Rab 18.

antibody. Additional nonspecific bands that were not removed by competition were also present. Immunoblots of mouse tissues (Figure 4.13) demonstrated strong immunoreactivity of the specific 29 kD band in brain, stomach, heart and spleen. Lower levels of immunoreactivity were seen in kidney cortex and medulla, small intestine and pancreas. Little or no immunoreactivity was seen in liver.

Immunolabeling of endogenous Rab 18 in MDCK cells demonstrated perinuclear staining in a portion of cells (Figure 4.14). These results are consistent with the immunolabeling seen in principal cells of the collecting duct.

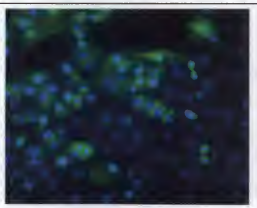

Figure 4.14. Rab 18 immunolabeling in MDCK cells.

Rab 18 immunostaining of mouse kidney (Figure 4.15, panels 1 and 3) was found in proximal and distal tubules of the cortex and medulla as well as CD by immunofluorescence. Colocalization with the V-ATPase E subunit (Figure 4.15, panels 2 and 5) was used to identify proximal tubule and CD. Merged images (Figure 4.15, panels 3 and 6) demonstrated that Rab 18 colocalized with the V-ATPase E subunit in apical borders of proximal tubule cells. In CD cells of the cortex and medulla, antibody to Rab 18 labeled principal cells not IC. Cells of cortical and medullary distal tubules devoid of V-ATPase E subunit staining were also positive for Rab 18.

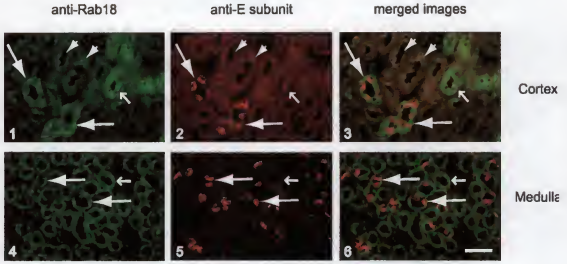

Figure 4.15. Representative immunolocalization of Rab 18 and the E subunit of V-ATPase in mouse kidney tissue sections. (1) Immunolabeling in cortex of Rab 18. Arrows identify collecting duct, small arrow points to distal tubule and arrowheads indicate proximal tubule. (2) Immunolabeling in same image as in 1 with anti-E subunit. Arrows, small arrows and arrowheads point to same structures as in 1. (3) Merged image of panels 1 and 2. Arrows, small arrows and arrowheads are as in 1. (4) Immunolabeling in medulla of Rab 18. Arrows point to collecting duct, small arrow indicates distal tubule. (5) Same image as in 4 immunolabeled for E subunit. Arrows and small arrows indicate same structures as in 4. (6) Merged image of panels 4 and 5. Arrows and small arrow indicate same structures as in 4 and 5. Bar is 100μm and is indicative of all panels.

Rab 20

Immunoblot analysis of mouse kidney cortex and medulla with Rab 20 antibody (Figure 4.16, lanes 1 and 2) showed strong specific immunoreactivity with a 32 kD polypeptide that was not present when anti-Rab 20

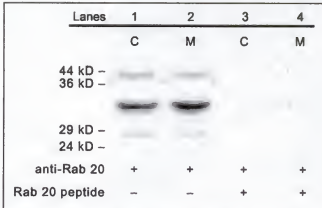

Figure 4.16. Immunoblotting with antibody to Rab 20. Homogenized kidney cortex (C) or medulla (M) tissue immunoblotted with anti-Rab 20 (lanes 1 and 2) or with anti-Rab 20 in the presence of the immunogenic peptide (lanes 3 and 4).

was co-incubated with its immunizing peptide (Figure 4.16, lanes 3 and 4). In addition to the band at 32 kD, immunoreactive bands were seen at slightly higher

Figure 4.17. Representative immunoblot of mouse tissues with antibody to Rab 20. Mouse tissues were homogenized and processed for immunoblotting as described in Figure 4.2 and in Materials and Methods with antibody to Rab 20.

than 36kD and slightly lower than 29kD in kidney cortex and kidney medulla. All the immunoreactive polypeptides were eliminated in immunoblots probed with antibody preincubated with the Rab 20 immunizing peptide, suggesting specificity. Mouse tissue immunoblots (Figure 4.17) demonstrated strong immunolabeling in liver, stomach, pancreas and spleen, and lower level of immunoreactivity in kidney cortex and medulla. Minimal levels were seen in brain and heart while small intestine did not appear to contain Rab 20 at detectable levels. Immunolabeling of Rab 20 in MDCK cells demonstrated diffuse cytoplasmic labeling including perinuclear localization (Figure 4.18).

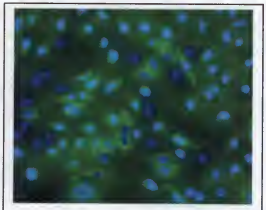

Figure 4.18. Rab 20 immunostaining in MDCK cells. MDCK cells were immunolabeled for Rab 20 and mounted with media containing DAPI to identify nuclei.

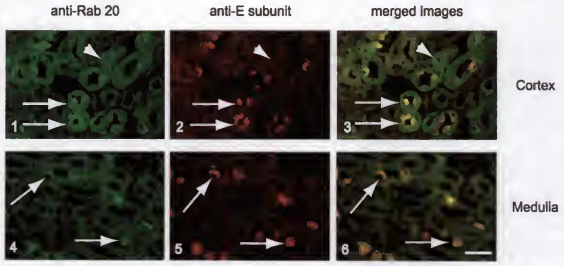

Figure 4.19. Representative immunolocalization of Rab 20 and the E subunit of V-ATPase in mouse kidney tissue sections. (1) Immunolabeling in cortex of Rab 20. Arrows identify collecting duct and arrowheads indicate distal tubule. (2) Immunolabeling with anti-E subunit in same image as in 1. Arrows and arrowheads point to same structures as in 1. (3) Merged image of panels 1 and 2. Arrows and arrowheads are as in 1. (4) Immunolabeling in medulla of Rab 20. Arrows point to collecting duct. (5) Same image as in 4 immunolabeled for E subunit. Arrows indicate same structures as in 4. (6) Merged image of panels 4 and 5. Arrows indicate same structures as in 4 and 5. Bar is 100μm and is indicative of all panels.

Dual immunofluorescence staining of mouse kidney (Figure 4.19) with antibody to Rab 20 (panels 1 and 3) and to V-ATPase E subunit (panels 2 and 5) demonstrated colocalization of Rab20 with V-ATPase E subunit in apical borders of intercalated cells of cortical (panels 1-3) and medullary (panels 4-6) CD (merged images, panels 3 and 6). Diffuse cytoplasmic staining of Rab20 in collecting ducts was also seen. In addition, Rab 20 labeling was observed in cortical tubules devoid of V-ATPase labeling (merged images).

In a preliminary examination of gestational rat kidneys (Figure 4.20), immunoreactivity of Rab 20 was absent at embryonic day (E) 16, but present in epithelial structures at E17. This immunolabeling for Rab 20 preceded by a day

the immunolabeling of E subunit. By E18 and E19, immunolabeling of Rab 20 was localized at or near plasma membrane and, at E20 and E21, was also cytoplasmic. E subunit labeling was slightly more intense at this stage and colocalization with Rab 20 could be seen.

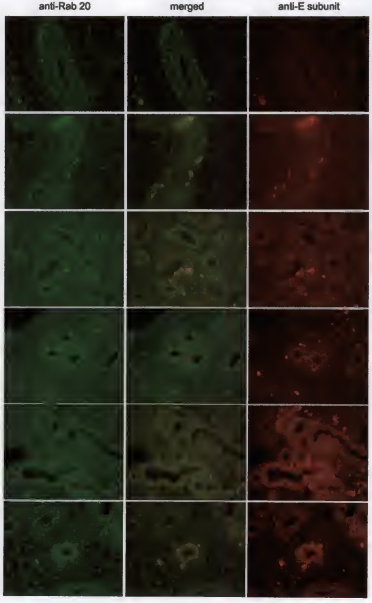

Figure 4.20. Representative images of Rab 20 and V-ATPase E subunit labeling in gestational mouse kidney sections. Mouse kidney sections from embryonic (E) mice were co-immunolabeled with anti-Rab 20 (green) and anti-E subunit (red). Merged images demonstrate colocalization.

Co-fractionation of Rab GTPases with V-ATPase

As a second, independent means of evaluating a colocalization of the V-ATPase E subunit with Rab GTPases in the mouse kidney, a differential centrifugation of homogenized mouse kidney was performed. Subsequently, the

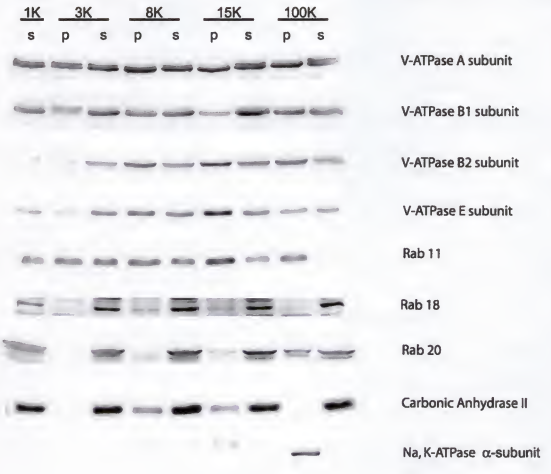

Figure 4.21. Differential centrifugation of mouse kidney medulla tissue. (s=supernatant; p=pellet)

different fractions were analyzed for the presence of V-ATPase subunits A, B1, B2 and E, Rabs 11, 18 and 20, and CAII and Na, K-ATPase α_1-subunit (Figure 4.21). The V-ATPase A subunit distributed in all fractions examined, although

some enrichment in pelleted membranes was observed. Distribution of the A subunit to the 15,000 x g (15K) membranes appeared to be of similar level to that of the 100,000 x g (100K) membrane fraction. The B1 and B2 V-ATPase subunit isoforms were also seen in all fractions, but segregated differentially to the 15K and 100K membranes. Whereas in membranes B1 subunit was predominantly located in the 100K pelleted fraction, the B2 subunit was localized slightly more in the 15K membrane fraction. The V-ATPase E-subunit was also found to be present in all fractions collected, however enrichment was observed preferentially in the 15K membrane fraction and to a lesser extent in the 100K membranes.

Since 15K and 100K membranes would be expected to contain plasma membrane and vesicle membranes, the presence or absence of Rabs in these fractions would likely indicate those that may be involved in the translocation of V-ATPase. Rab 11 was found to be more abundant in the 15K membrane fraction, although all pelleted fractions including the 100K membrane fraction demonstrated significant labeling for Rab 11 also. Strikingly, Rab 18 was found to predominate in supernatant fractions at all g-force levels. Some Rab 18 was found in pelleted membranes at 8,000 x g (8K) and 15K, however very little Rab 18 was pelleted at 100K. This pattern of distribution between 15K and 100K membranes is similar to the pattern seen for the B2 and E subunits of V-ATPase. As with Rab 18, significant levels of Rab 20 remained in supernatant fractions, pelleting minimally with the 15K membranes and slightly more so in the 100K membranes. The distribution of Rab 20 to the 100K membranes to a larger extent than to the 15K membranes is a similar pattern to the distribution of the V-

ATPase B1 subunit in these membrane fractions. As expected, CAII was largely found in the supernatants of the differential centrifugation steps. Immunoblotting for the Na, K-ATPase α_1-subunit demonstrated a strong immunoreactive polypeptide in the 100K membranes while only minimal amounts were present in the lower g-force fractions. These results indicate similar segregation pattern of Rab 11 and 18 with the V-ATPase B2 and E subunits in plasma membrane fractions, while Rab 20 appears to segregate to plasma membrane fractions containing more V-ATPase B1 subunit.

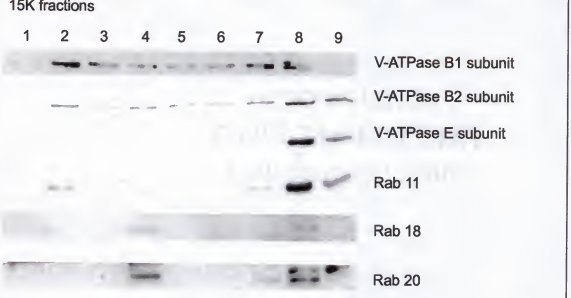

Figure 4.22. Immunoblots of Percoll gradent fractions from 15K membranes. Fractions are of increasing density.

To examine the varying patterns of the Rab GTPases observed in the 15K and 100K pelleted differential centrifugation fractions enriched in V-ATPase, Percoll gradients were run on these fractions. In Percoll gradients of 15K membranes (Figure 4.22), the V-ATPase B subunit isoforms were present in

nearly all fractions. The B1 isoform was highest in fractions 2, 7 and 8, corresponding to densities of 1.018 g/ml (#2) and 1.033 g/ml (#7) as determined by density marker beads run in parallel to the experimental samples. The B2 isoform was highest in fractions 8 and 9, corresponding to densities of 1.049-1.121 g/ml (#9), with lower levels seen in fractions 7 and 2. The V-ATPase E subunit was only found in fractions 8 and 9. Similarly, Rab 11 was highest in fraction 8, although significant levels of Rab 11 were found in fractions 9, 7 and

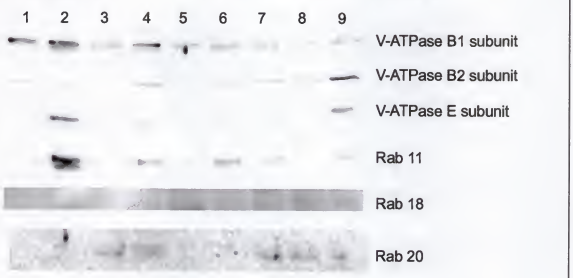

Figure 4.23. Immunoblots of Percoll fractions from 100K membranes. Fractions are of increasing density.

2. Membrane-bound Rab 18 and Rab 20 were segregated to fractions 4 and 8.

As with the 15K membranes, B1 subunit isoform in Percoll gradient fractions from 100K membranes (Figure 4.23) was preferentially found in fractions 1, 2 (1.018 g/ml) and 4, although all fractions contained some B1 isoform. The B2 isoform was also in most Percoll fractions, but was abundant in fraction 9 (1.049-1.121 g/ml). The V-ATPase E subunit was detected mostly in

fractions 2 (1.018 g/ml) and 9 (1.049-1.121 g/ml) of Percoll gradients of 100K membranes. Rab 11 demonstrated a similar pattern as the E subunit, although most of this protein was present in fraction 2 (1.018 g/ml). Rab 18 was undetectable in Percoll gradient fractions of 100K membranes. Minimal levels of Rab 20 were detected in lower density fractions 3 and 4 and in higher density fractions 7, 8 and 9, The gradient results indicate significant co-migration of these Rab GTPases with the V-ATPase subunits.

CHAPTER 5
CONCLUSIONS

Angiotensin II Effects on Apoptosis

The results of the developmental studies and angiotensin did not provide any support for the hypothesis that the RAS is involved in the regulation of apoptosis during the differentiation of the loop of Henle and the collecting duct (CD). The *in vivo* study demonstrated no effects on apoptosis in the loop of Henle or in the CD following administration of Losartan or PD123319, inhibitors of the type 1 (AT_1R) and type 2 (AT_2R) angiotensin II (Ang) receptors, respectively. Further, no demonstrable changes were seen in cell proliferation in these animals. Interestingly, pups from one out of the four litters studied were much smaller than those from the other litters and had smaller kidneys with less developed papillae. In pups from that litter, treatment with Losartan was unexpectedly associated with a decrease in the apoptotic index and little evidence of epithelial transformation, suggesting that Losartan might delay the onset of the apoptotic process. To test this hypothesis would require prenatal exposure to Losartan. There was no effect of Losartan on pups from any of the other litters.

The lack of a direct effect of Ang receptor inhibitors on apoptosis and renal tubule differentiation is also supported by recent observations in Ang receptor knockout mice. Double nullizygotes of the AT_1a and AT_1b angiotensin II receptors were shown to have a similar phenotype to that of animals that are homozygous

for the angiotensinogen null mutation. In both of these models a decreased papillary size as well as delayed glomerular development and hyperplasia of the vasculature were described [33, 98], however, these changes were not observed until 3 weeks of age. An AT_2R null animal model was not found to have any differences in the numbers of apoptotic cells in the embryonic kidneys. Further, developmental maturity was assessed as the same between the AT_2R knockout and wild type animals [99]. Only under abnormal conditions was any difference found in the developing renal medulla [100] in these AT_2R null mutant mice. These findings indicate that the developmental regulation of apoptosis in the loop of Henle and CD do not involve the AT_2R as was hypothesized.

AT_2R have been identified in the mesenchymal cells in developing kidney and ureter and in interstitial cells of the renal medulla [101, 31]. In the AT_2R null mutant mice, physical restriction of the ureter has been attributed to a decreased apoptosis in the ureter [102]. It is conceivable that changes in the cellular makeup of this tissue may alter the process of excretion of urine. Malformations of the renal papilla may be a secondary effect of the abnormal excretory system.

The *in vitro* studies further corroborate the suggestion that the effect of Ang on apoptosis in renal epithelium is indirect. In response to a range of concentrations of Ang, no demonstrable changes in cell proliferation or cell death were found. With the blockade of either the AT_1R or the AT_2R, no differences could be seen in these processes. The *in vitro* data would suggest that the effects of Ang on the renal papilla may be indirect.

Thus, the combined data from the *in vivo* and *in vitro* studies indicate that in the renal epithelium of the ascending limb of the loop of Henle and in IC, apoptosis is not directly mediated by the actions of Ang. It is conceivable that other factors or changes that are occurring in the renal papilla during the first postnatal week are responsible for the apoptotic wave evident in the developing rat renal papilla. Such factors may include glucocorticoid signaling or changes in osmotic gradients. Additionally, the vasculature of the rat renal papilla undergoes changes during this time [103], which may serve to alter the availability or concentrations of growth factors or other molecules in the renal papilla. Inhibition of the V-ATPase has been shown to induce apoptosis in several cell types [36, 37, 39, 40, 41, 42, 104]. Intercalated cells (IC) of the kidney CD express high levels of the V-ATPase at either the apical (α cells) or the basolateral (β cells) membrane and, thus, inhibition of the V-ATPase may contribute to the apoptosis of these cells seen in the developing CD. Neonatal animals have limited ability to regulate acid-base balance and IC characteristics, and presumably function, change during this time. The level and activity of the V-ATPase are dramatically increased in the first postnatal weeks. A better understanding of the regulation of the V-ATPase would provide a framework for examining the role of the V-ATPase in the wave of developmental apoptosis in the kidney.

Rab GTPases in Adult Mouse Kidney

Examination of Rabs 5a, 11, 13, 18 and 20 in mouse kidney indicates cell-specific localization within the tubule epithelium and colocalization or co-migration with the V-ATPase. Rab 11 colocalizes with the V-ATPase in the apical

regions of proximal tubule cells, which preferentially express the B2 subunit of V-ATPase. Similarly the majority of membrane-bound Rab 11 segregated with the B2 subunit although some Rab 11 was distributed with the B1 subunit. Rab 18 colocalized with the V-ATPase in proximal tubule cells as well and segregated more with the B2 subunit than the B1 subunit in the biochemical analysis. Rab 20 behaved in contrast to Rabs 11 and 18, colocalizing with the V-ATPase in IC, which was consistent with its preferred segregation with the B1 subunit over the B2 subunit of the V-ATPase in the biochemical analysis. Thus this Rab GTPase may play a role in V-ATPase trafficking in IC. Rabs 5a and 13 did not colocalize specifically with the V-ATPase and were ruled out as candidates for involvement in V-ATPase trafficking.

Significant diversity in tissue expression is seen with Rab 11, although high levels in kidney, brain and stomach may underlie a specialized role for Rab 11 in these tissues. Presenilins, proteins that are altered in autosomal dominant early-onset Alzheimer's disease, have been recently shown to interact with the c-terminus of Rab 11 [105]. In gastric parietal cells, a secretory epithelia, histamine administration coincided with relocalization of the H, K-ATPase along with Rab 11 [83]. Previously, Rab 11 was localized in rabbit kidney primarily in apical regions of CD cells and "thin cortical tubules" while no significant staining was seen in glomeruli or proximal tubule. In this study, staining in mouse kidney tissues demonstrated significant immunostaining in apical regions of principal cells of the CD and connecting tubule. Some staining was noted in apical borders of proximal tubule cells, which was recapitulated in neonatal mice. The

differences seen in this study relative to that of the rabbit kidney may indicate differences in the species or in the methodologies used. The localization of Rab 11 to apical regions of distal convoluted and proximal tubule cells is interesting as these segments contain receptors for estrogen [106] or are responsive to altered estrogen levels [107]. Rab 11 mRNA in rat uterus has been shown to be induced in response to estrogen administration [86]. The differential expression of Rab 11 in proximal tubule and not in the IC of the CD is also noteworthy as these two sites exhibit different expression patterns for the two isoforms of the B-subunit of the V-ATPase [49], which has been suggested to indicate the potential for differential regulation of the V-ATPase. Biochemical analyses of Rab 11 indicate two populations of membrane-bound Rab 11. Consistently, the Rab 11 present in the 15K membranes segregated with the V-ATPase B2 subunit isoform fractions of higher density, while Rab 11 in the 100K membranes was found predominantly at lower density along with the V-ATPase B1 subunit isoform. The localization of Rab 11 in proximal tubule cells, which contain abundant plasma membrane V-ATPase with the B2 subunit isoform, is consistent with the majority of Rab 11 fractionating with the B2 subunit isoform in 15K and 100K membranes. The identification of membrane-bound Rab 11 in low density fractions along with the V-ATPase B1 subunit isoform may indicate a different role for this population of Rab 11 in the kidney.

Immunolabeling for Rab 18 in proximal tubule cells is similar to that of a previous study [89] where Rab 18 was identified in vesicular structures below the apical brush border of proximal tubule cells by fluorescence and immunoelectron

microscopy. The localization of Rab 18 to principal cells of the CD is consistent with the finding of apical staining in CD as reported by Lütcke et al. [89], however they did not find this staining in medullary regions. The differences between the two studies may reflect different methodologies. The minimal expression of Rab 18 seen in kidney cortex and medulla relative to tissues with high expression may indicate a limited, although perhaps specialized role for Rab 18 in the kidney. Differential centrifugation of mouse kidney demonstrated that the majority of Rab 18 is not membrane bound as a significant portion of the Rab 18 remained in the supernatant fraction of the 100K centrifugation. The localization of Rab 18 throughout the cytosol in cortical and medullary tubules and CD is in agreement with this segregation and may represent an inactive pool of Rab 18. Although most of the Rab 18 was found in supernatant fractions, some did pellet in the 8K and 15K centrifugations. The presence of Rab 18 in the 15K pellet, where the B2 subunit isoform and E subunit of the V-ATPase were most abundant, comports with the colocalization of Rab 18 with the V-ATPase E subunit in apical regions of the proximal tubule, a region which contains prominent plasma membrane V-ATPase B2 subunit isoform. Elucidation of the specific function of Rab 18 awaits further study.

The expression of Rab 20 in mouse tissues seen in this study largely recapitulates the distribution of Rab 20 mRNA [89]. Strong immunostaining of Rab 20 in mouse kidney was identified in apical regions of α IC where it was found to co-localize with the V-ATPase. Additional diffuse staining above background levels seen in tubules of the cortex not labeled for V-ATPase is more

restricted than that described by Lütcke et al. [89], which may be due to differences in the methods that were used. Ubiquitous labeling of cytoplasm in cortical epithelia was seen in gestational rat kidneys although clear membranous labeling and increasing cytoplasmic labeling was seen after E17. This localization pattern is similar to the adult. The colocalization of Rab 20 with V-ATPase in IC is intriguing and suggests that Rab 20 may be involved in the translocation of V-ATPase in response to physiological stimulation. The localization of Rab 20 to the cytosol of CD cells is reflected in the differential centrifugation, where high levels of Rab 20 were segregated to supernatant fractions. As with Rab 11, the patterns of segregation of Rab 20 on gradients would imply differing populations of membrane-bound Rab 20. The portion of Rab 20 pelleted at 15K was found in fractions of higher density coinciding with the pattern of localization of the V-ATPase B2 subunit isoform and E subunit, and Rab 11. Rab 20 from the 100K membranes was preferentially found at both lower and higher densities, which coincided with the presence of the V-ATPase B1 and B2 subunit isoforms, respectively. Further study will be necessary to establish the role of Rab 20 in cells of the CD and other regions of the nephron.

The ubiquitous labeling for Rab 5a in proximal and distal nephron as well as in CD cells in mouse kidney sections and in MDCK cells is consistent with the important role of Rab 5 in endocytosis [67, 68, 69]. Renal tubules support significant lumen-to-intracellular as well as transcellular processes via apical integral membrane proteins, many of which are regulated in part by endocytic removal from the plasma membrane. The tissue expression seen in these

experiments is indicative of a universal role for Rab 5a as it was detected in nearly all of the tissues studied. The widespread expression pattern of this Rab GTPase would suggest that Rab 5a likely does not play a specific role in the translocation of the V-ATPase from intracellular sites to the plasma membrane during physiological regulation, although a role for Rab 5a in the removal of the V-ATPase from the plasma membrane cannot be ruled out.

The findings of this study also eliminate the involvement of Rab 13 in the trafficking of V-ATPase. Rab 13 has previously been demonstrated at low levels in mouse intestine, kidney, liver, and endothelial cells at junctional complexes [88]. In cell culture, Rab 13 co-localizes with zonula occludens 1 (ZO-1), a tight junction protein [88]. In this study, immunoblotting demonstrated low levels of Rab 13 in various tissues including kidney, although high levels were observed in brain. Very little expression of Rab 13 was identified in liver and small intestine, which may be a result of the limitation of this technique in identifying low levels of expression in these tissues. Rab 13 immunolabeling was identified in apical regions of thick ascending limb cells of mouse kidney. The function of Rab 13 is unknown, however, its previous localization to junctional complexes and colocalization with ZO-1 leads to the speculation that Rab 13 may be involved in regulating paracellular transport in these tubules by regulating the junctional complex. Paracellular transport of magnesium is important in this region of the nephron [108]. An understanding of the role of Rab 13 in the kidney awaits further study.

This examination of select Rab GTPases demonstrates a tissue- and cell-specific distribution of these proteins in the mouse kidney. Colocalization of Rab GTPases with the V-ATPase subunits by immunolocalization as well as biochemical methods demonstrates that Rabs 11, 18 and 20 are, in part, present in association with the V-ATPase. Rabs 5a and 13 do not appear to specifically associate with the V-ATPase in mouse kidney. These results identify a subset of Rab GTPases that are potentially important in the regulated trafficking of the V-ATPase and warrant further study under physiological conditions.

CHAPTER 6
FUTURE DIRECTIONS

Although Ang was not found to be involved in the regulation of the developmental wave of apoptosis in the renal medulla, several other possibilities of exploration remain. One intriguing possibility is the regulation of the V-ATPase. The adult TAL cells exhibit some plasma membrane V-ATPase labeling, whereas the thin ascending limb does not. Additionally, the only cells that are lost from the developing CD are those that have extensive plasma membrane V-ATPase. Since the wave of apoptosis is halted at the border of inner and outer medulla, it is reasonable that the proximal tubule is not affected by the signals that induce loss of cells containing plasma membrane V-ATPase. The absolute consistency of the formation of the border between the inner and outer medulla would suggest that either a second signal or the establishment of extracellular conditions by this time in neonatal development serve to stop the apoptotic wave. Although V-ATPase is expressed in neonatal animals, its activity is known to increase during the first postnatal weeks. The potential role of Rab GTPases in the trafficking of the V-ATPase as a means of regulating acid-base transport and any collateral effects demonstrated during renal development warrants examination.

In order to further examine the role of Rab GTPases in the regulation of V-ATPase, several experiments would be instructive. As the only known model of *in vivo* movement of the V-ATPase is acid-loading of animals, examination of the

relocalization of candidate Rab GTPases under such physiological alteration is necessary as an initial evaluation of the functional interaction. The identification of protein components present in V-ATPase-positive vesicles would be informative as to the mechanism of its transport. The use of *in vitro* Rab GTPase overexpression models to examine V-ATPase translocation is also intriguing. Finally, to address the role of V-ATPase in developmental apoptosis, the findings regarding the regulation of V-ATPase in the adult should be evaluated in the gestational and neonatal kidney.

Administration of NH_4Cl in animal models of acidosis using rats and rabbits has been shown to induce a relocalization of V-ATPase independently of protein or mRNA synthesis. If the candidate Rab GTPases are involved in the relocalization of the V-ATPase, the expectation would be that the candidate Rabs would be similarly relocated. This relocalization of Rab GTPases could be examined both by immunolabeling of kidney sections from acid-loaded and control animals as well as by segregation assays (differential centrifugation, Percoll gradients) as used in this dissertation. Such findings would provide evidence of *in vivo* relevance.

This dissertation was able to establish a different segregation pattern of V-ATPase fractions exhibiting more of one or the other of the B subunits, which have differential expression in renal cells containing abundant plasma membrane V-ATPase. An identification of component proteins in these differing populations of membrane fractions may provide insight into the differential regulation of the two configurations of V-ATPase. An extraction of the differing populations of V-

ATPase fractions might be obtained through immunoprecipitation of the V-ATPase via antibodies that specifically recognize each of the two B subunits, the B1 and B2 at 56kD and 58kD, respectively. Using both SDS-PAGE and immunoblotting for specific known components of the SNARE complex, the identity of potential regulatory interactions between vesicles and plasma membrane regions may be ascertained. Additionally, the presence of unknown immunoreactive polypeptides might indicate potential binding partners to the candidate Rab GTPases. Identification of these immunoreactive polypeptides through sequencing may lead to the discovery of effector molecules for Rabs 18 and 20, currently unknown. An interaction between any of these proteins and the candidate Rab GTPases could be further examined by co-immunoprecipitation from the V-ATPase-enriched fractions or by yeast two-hybrid assays.

Only one experimental model of *in vitro* movement of the V-ATPase has been described in cultured rat inner medullary collecting duct cells [109, 110]. Using this model, several components of potential SNARE complexes have been identified [111, 112]. This model could be explored in renal epithelial cells such as MDCK to investigate the presence of Rab GTPases and their effectors by immunolocalization studies as described in this dissertation as well as by immunoblotting. As an alternative means of exploring V-ATPase movement, identification of translocation of V-ATPase as a consequence of overexpression of dominant positive (GTPase-deficient) or dominant negative (GTP-binding deficient) would be informative. Several Rab GTPases, including Rab 5 and Rab 11, have been examined using these constructs modeled after Ras mutants [77,

76, 68]. Finding a correlation between loss-of-function or gain-of-function Rab GTPase mutants and alterations in localization of V-ATPase may indicate a functional interaction between these Rab GTPases and the V-ATPase. Further, examination of cells expressing these constructs under conditions that induce apoptosis may provide insight into the role of regulation of V-ATPase trafficking, as opposed to enzyme inhibition, in the apoptotic process.

Finally, in order to examine the role of these Rab GTPases in the regulation of the developmental apoptotic wave in the kidney, the expression and localization of these Rab GTPases as well as any supporting proteins need to be localized in gestational and neonatal kidney tissue. The expression patterns may provide clues as to the role of V-ATPase regulation in the apoptotic wave seen in the neonatal kidney.

Establishing the proteins present in V-ATPase-positive vesicles and, further, specifically examining the role of Rab GTPases in the regulated trafficking of the V-ATPase will give insight into mechanisms of control of both cellular and systemic acid-base regulation. Ultimately, understanding the mechanisms surrounding the regulation of V-ATPase activity and its role in apoptosis may provide a basis for developing pharmacological intervention in physiological alterations of acid-base regulation as well as further the understanding of the developmental processes in the kidney.

LIST OF REFERENCES

1. Hurle, J.M., *Cell death in developing systems.* Meth Acheiv Exp Pathol, 1988. **13**: p. 55-86.

2. Saunders, J.W., Jr., *Death in embryonic systems.* Science, 1966. **154**: p. 604-612.

3. Koseki, C., D. Herzlinger, and Q. Al-Awqati, *Apoptosis in metanephric development.* J Cell Biol, 1992. **119**(5): p. 1327-1333.

4. Coles, H.S.R., J.F. Burne, and M.C. Raff, *Large-scale normal cell death in the developing rat kidney and its reduction by epidermal growth factor.* Development, 1993. **118**: p. 777-784.

5. Kim, J., G.-S. Lee, C.C. Tisher, and K.M. Madsen, *Role of apoptosis in development of the ascending thin limb of the loop of Henle in rat kidney.* Am J Physiol, 1996. **271**: p. F831-F845.

6. Kim, J., J.-H. Cha, C.C. Tisher, and K.M. Madsen, *Role of apoptotic and nonapoptotic cell death in removal of intercalated cells from developing rat kidney.* Am J Physiol, 1996. **270**: p. F575-F592.

7. Kahane, V.L., J.C. Cutrin, C.P. Stetton, M. del Carment Fernandez, S.D. Catz, and N.B. Sterin-Speziale, *Biochemical and morphological changes in the developing kidney.* Biol Neonate, 1995. **68**: p. 141-152.

8. Orellana, S.A. and E.D. Avner, *Cell and molecular biology of kidney development.* Sem Nephrol, 1998. **18**(3): p. 233-243.

9. Baum, M. and R. Quigley, *Maturation of proximal tubular acidification.* Pediatr Nephrol, 1993. **7**(6): p. 785-791.

10. Kim, J., C.C. Tisher, and K.M. Madsen, *Differentiation of intercalated cells in developing rat kidney: an immunohistochemical study.* Am J Physiol, 1994. **266**(6 Pt 2): p. F977-F990.

11. Numata, M., S. Ohkuma, and S. Iseki, *Expression and localization of mRNA for the 16 KD subunit of V-ATPase in the rat embryo.* J Histochem Cytochem, 1995. **43**(8): p. 761-769.

12. Karashima, S., S. Hattori, T. Ushijima, A. Furuse, H. Nakazato, and I. Matsuda, *Developmental changes in carbonic anhydrase II in the rat kidney.* Pediatr Nephrol, 1998. **12**(4): p. 263-268.

13. McKenzie, J., J. Scott, and T. Inagami, *Immunohistochemical localization of atrial natriuretic peptide in the developing and adult mammalian kidney.* Am J Anat, 1991. **190**(2): p. 182-191.

14. Holthofer, H., *Ontogeny of cell type-specific enzyme reactivities in kidney collecting ducts.* Pediatr Res, 1987. **22**(5): p. 504-508.

15. Holthofer, H., *Cell type-specific glycoconjugates of collecting duct cells during maturation of the rat kidney.* Cell Tissue Res, 1988. **253**(2): p. 305-309.

16. Gomez, R.A., *Molecular biology of components of the renin-angiotensin system during development.* Pediatr Nephrol, 1990. **4**: p. 421-423.

17. Wang, D.H., Y. Du, H. Zhao, J.P. Granger, R.C. Speth, and D.J. Dipette, *Regulation of angiotensin type 1 receptor and its gene expression: Role in renal growth.* J Am Soc Nephrol, 1997. **8**: p. 193-198.

18. Tufro-McReddie, A., D.W. Johns, K.M. Geary, H. Dagli, A.D. Everett, R.J. Chevalier, R.M. Carey, and R.A. Gomez, *Angiotensin II type 1 receptor: role in renal growth and gene expression during normal development.* Am J Physiol, 1994. **266**: p. F911-F918.

19. Wolf, G., F.N. Ziyadeh, G. Zahner, and R.A.K. Stahl, *Angiotensin II is mitogenic for cultured rat glomerular endothelial cells.* Hypertension, 1996. **27**: p. 897-905.

20. Wolf, G., F.N. Ziyadeh, U. Helmchen, G. Zahner, R. Schroeder, and R.A. Stahl, *ANG II is a mitogen for a murine cell line isolated from medullary thick ascending limb of Henle's loop.* Am J Physiol, 1995. **268**: p. F940-F947.

21. Nakajima, M., H.G. Hutchinson, M. Fujinaga, W. Hayashida, R. Morishita, L. Zhang, M. Horiuchi, R.E. Pratt, and V.J. Dzau, *The angiotensin II type 2 (AT2) receptor antagonizes the growth effects of the AT1 receptor: Gain-of-function study using gene transfer.* Proc Nat Acad Sci, 1995. **92**: p. 10663-10667.

22. Stoll, M., U.M. Steckelings, M. Paul, S.P. Bottari, R. Metzger, and T. Unger, *The angiotensin AT2-receptor mediates inhibition of cell proliferation in coronary endothelial cells.* J Clin Invest, 1995. **95**: p. 651-657.

23. Tsuzuki, S., T. Matoba, S. Eguchi, and T. Inagami, *Angiotensin II type 2 receptor inhibits cell proliferation and activates tyrosine phosphatase.* Hypertension, 1996. **28**: p. 916-918.

24. Yamada, T., M. Horiuchi, and V.J. Dzau, *Angiotensin II type 2 receptor mediates programmed cell death.* Proc Nat Acad Sci, 1996. **93**: p. 156-160.

25. Terada, Y., K. Tomita, H. Nonoguchi, and F. Marumo, *PCR localization of angiotensin II receptor and angiotensinogen mRNAs in rat kidney.* Kidney Int, 1993. **43**: p. 1251-1259.

26. Norwood, V.F., M.R. Craig, J.M. Harris, and R.A. Gomez, *Differential expression of angiotensin II receptors during early renal morphogenesis.* Am J Physiol, 1997. **272**: p. R662-R668.

27. Aguilera, G., S. Kapur, P. Feuillan, B. Sunar-Akbasak, and A.J. Bathia, *Developmental changes in angiotensin II receptor subtypes and AT1 receptor mRNA in rat kidney.* Kidney Int, 1994. **46**: p. 973-979.

28. Mujais, S.K., S. Kauffman, and A.I. Katz, *Angiotensin II binding sites in individual segments of the rat nephron.* J Clin Invest, 1986. **77**: p. 315-318.

29. Kakuchi, J., T. Ichiki, S. Kiyama, B.L.M. Hogan, A. Fogo, T. Inagami, and I. Ichikawa, *Developmental expression of renal angiotensin II receptor genes in the mouse.* Kidney Int, 1995. **47**: p. 140-147.

30. Ozono, R., Z. Wang, A.F. Moore, T. Inagami, H.M. Siragy, and R.M. Carey, *Expression of the subtype 2 angiotensin (AT_2) receptor protein in rat kidney.* Hypertension, 1997. **30**: p. 1238-1246.

31. Shanmugam, S., C. Llorens-Cortes, E. Clauser, P. Corvol, and J.-M. Gasc, *Expression of angiotensin II AT2 receptor mRNA during development of rat kidney and adrenal gland.* Am J Physiol, 1995. **268**: p. F922-F930.

32. Niimura, F., P.A. Labosky, J. Kakuchi, S. Okubo, H. Yoshida, T. Oikawa, T. Ichiki, A.J. Naftilan, A. Fogo, T. Inagami, B.L.M. Hogan, and I. Ichikawa, *Gene targeting in mice reveals a requirement for angiotensin in the development and maintenance of kidney morphology and growth factor regulation.* J Clin Invest, 1995. **96**: p. 2947-2954.

33. Nagata, M., K. Tanimoto, A. Fukamizu, Y. Kon, F. Sugiyama, K. Yagami, K. Murakami, and T. Watanabe, *Nephrogenesis and renovascular development in angiotensinogen-deficient mice.* Lab Invest, 1996. **75**: p. 745-753.

34. McCausland, J.E., G.B. Ryan, and D. Alcorn, *Angiotensin converting enzyme inhibition in the postnatal rat results in decreased cell proliferation in the renal outer medulla.* Clinical and Experimental Pharmacology amd Physiology, 1996. **23**: p. 552-554.

35. Guron, G., M.A. Adams, B. Sundelin, and P. Friberg, *Neonatal angiotensin-converting enzyme inhibition in the rat induces persistent abnormalities in renal function and histology.* Hypertension, 1997. **29**: p. 91-97.

36. Long, X., M.T. Crow, S.J. Sollott, L.O. O'Neill, D.S. Menees, M. de Lourdes Hipolito, M.O. Boluyt, T. Asai, and E.G. Lakatta, *Enhanced expression of p53 and apoptosis induced by blockade of the vacuolar proton ATPase in cardiomyocytes.* J Clin Invest, 1998. **101**(6): p. 1453-1461.

37. Otani, H., T. Yamamura, Y. Nakao, R. Hattori, H. Fujii, H. Ninomiya, M. Kido, H. Kawaguchi, M. Osako, H. Imamura, T. Ohta, and S. Ohkuma, *Vacuolar H(+)-ATPase plays a crucial role in growth and phenotypic modulation of myofibroblasts in cultured human saphenous vein.* Circulation, 2000. **102**(19 Suppl 3): p. III269-III274.

38. Ishisaki, A., S. Hashimoto, T. Amagasa, and T. Nishihara, *Caspase-3 activation during the process of apoptosis induced by a vacuolar type H(+)-ATPase inhibitor.* Biol Cell, 1999. **91**(7): p. 507-513.

39. Hashimoto, S., A. Ishisaki, K. Yamato, K. Aiko, T. Amagasa, and T. Nishihara, *Intracellular apoptosis-inducing factor is induced by a vacuolar type H+-ATPase inhibitor in B lineage cells.* J Cell Physiol, 2001. **186**(1): p. 65-72.

40. Okahashi, N., I. Nakamura, E. Jimi, M. Koide, T. Suda, and T. Nishihara, *Specific inhibitors of vacuolar H(+)-ATPase trigger apoptotic cell death of osteoclasts.* J Bone Miner Res, 1997. **12**(7): p. 1116-1123.

41. Ohta, T., H. Arakawa, F. Futagami, S. Fushida, H. Kitagawa, M. Kayahara, T. Nagakawa, K. Miwa, K. Kurashima, M. Numata, Y. Kitamura, T. Terada, and S. Ohkuma, *Bafilomycin A1 induces apoptosis in the human pancreatic cancer cell line Capan-1.* J Pathol, 1998. **185**(3): p. 324-330.

42. Karwatowska-Prokopczuk, E., J.A. Nordberg, H.L. Li, R.L. Engler, and R.A. Gottlieb, *Effect of vacuolar proton ATPase on pHi, Ca2+, and apoptosis in neonatal cardiomyocytes during metabolic inhibition/recovery.* Circ Res, 1998. **82**(11): p. 1139-1144.

43. Niessen, H., G.W. Meisenholder, H.L. Li, S.L. Gluck, B.S. Lee, B. Bowman, E.R. L, B.M. Babior, and G.R. A, *Granulocyte colony-stimulating factor upregulates the vacuolar proton ATPase in human neutrophils.* Blood, 1997. **90**(11): p. 4598-4601.

44. Gottlieb, R., H. Giesing, J. Zhu, R. Engler, and B. Babior, *Cell acidification in apoptosis: granulocyte colony-stimulating factor delays programmed cell death in neutrophils by up-regulating the vacuolar H(+)-ATPase.* Proc Nat Acad Sci, 1995. **92**(13): p. 5965-5968.

45. Stevens, T.H. and M. Forgac, *Structure, function and regulation of the vacuolar (H+)-ATPase.* Annu Rev Cell Dev Biol, 1997. **13**: p. 779-808.

46. Gluck, S.L., D.M. Underhill, M. Iyori, L.S. Holliday, T.Y. Kostrominova, and B.S. Lee, *Physiology and biochemistry of the kidney vacuolar H+-ATPase.* Annu Rev Physiol, 1996. **58**: p. 427-445.

47. Forgac, M., *Structure and properties of the vacuolar (H+)-ATPases.* J Biol Chem, 1999. **274**(19): p. 12951-12954.

48. Wilkens, S., E. Vasilyeva, and M. Forgac, *Structure of the vacuolar ATPase by electron microscopy.* J Biol Chem, 1999. **274**(45): p. 31804-31810.

49. Nelson, R.D., X.-L. Guo, K. Masood, D. Brown, M. Kalkbrenner, and S. Gluck, *Selectively amplified expression of an isoform of the vacuolar H^+-ATPase 56-kilodalton subunit in renal intercalated cells.* Proc Nat Acad Sci, 1992. **89**: p. 3541-3545.

50. Bernasconi, P., T. Rausch, I. Struve, L. Morgan, and L. Taiz, *An mRNA from human brain encodes an isoform of the B subunit of the vacuolar H(+)-ATPase.* J Biol Chem, 1990. **265**(29): p. 17428-17431.

51. Sudhof, T., V. Fried, D. Stone, P. Johnston, and X. Xie, *Human endomembrane H+ pump strongly resembles the ATP-synthetase of Archaebacteria.* Proc Nat Acad Sci, 1989. **86**(16): p. 6067-6071.

52. Nelson, H., S. Mandiyan, and N. Nelson, *A bovine cDNA and a yeast gene (VMA8) encoding the subunit D of the vacuolar H^+-ATPase.* Proc Nat Acad Sci, 1995. **92**(2): p. 497-501.

53. Zhang, K., Z. Wang, and S. Gluck, *Identification and partial purification of a cytosolic activator of vacuolar H(+)-ATPases from mammalian kidney.* J Biol Chem, 1992. **267**(14): p. 9701-9705.

54. Zhang, K., Z. Wang, and S. Gluck, *A cytosolic inhibitor of vacuolar H(+)-ATPases from mammalian kidney.* J Biol Chem, 1992. **267**(21): p. 14539-14542.

55. Blair, H.C., S.L. Teitelbaum, R. Ghiselli, and S. Gluck, *Osteoclastic bone resorption by a polarized vacuolar proton pump.* Science Wash DC, 1989. **245**: p. 855-857.

56. Nanda, A., J.H. Brumell, T. Nordstrom, L. Kjeldsen, H. Sengelov, N. Borregaard, O.D. Rotstein, and S. Grinstein, *Activation of proton pumping in human neutrophils occurs by exocytosis of vesicles bearing vacuolar-type H+-ATPases.* J Biol Chem, 1996. **271**(27): p. 15963-15970.

57. Bastani, B., H. Purcell, P. Hemken, D. Trigg, and S. Gluck, *Expression and distribution of renal vacuolar proton-translocating adenosine triphosphatase in response to chronic acid and alkali loads in the rat.* J Clin Invest, 1991. **88**: p. 126-136.

58. Verlander, J.W., K.M. Madsen, J.K. Canon, and C.C. Tisher, *Activation of acid-secreting intercalated cells in rabbit collecting duct with ammonium chloride loading.* Am J Physiol, 1994. **266**(4 Pt 2): p. F633-F645.

59. Olkkonen, V.M. and H. Stenmark, *Role of Rab GTPases in membrane traffic.* Int Rev Cytol, 1997. **176**: p. 1-85.

60. Takai, Y., T. Sasaki, and T. Matozaki, *Small GTP-binding proteins.* Physiol Rev, 2001. **81**(1): p. 153-208.

61. Rothman, J.E., *Mechanisms of intracellular protein transport.* 372, 1994. **6501**: p. 55-63.

62. Halachmi, N. and Z. Lev, *The Sec1 family: a novel family of proteins involved in synaptic transmission and general secretion.* J Neurochem, 1996. **66**(3): p. 889-97.

63. Haynes, L.P., A. Morgan, and R.D. Burgoyne, *nSec-1 (munc-18) interacts with both primed and unprimed syntaxin 1A and associates in a dimeric complex on adrenal chromaffin granules.* Biochem J, 1999. **342**(Pt 3): p. 707-14.

64. Yang, B., M. Steegmaier, L.C. Gonzalez, Jr, and R.H. Scheller, *nSec1 binds a closed conformation of syntaxin1A.* J Cell Biol, 2000. **148**(2): p. 247-52.

65. Waters, M.G. and F.M. Hughson, *Membrane tethering and fusion in the secretory and endocytic pathways.* Traffic, 2000. **1**(8): p. 588-97.

66. Grote, E., C.M. Carr, and P.J. Novick, *Ordering the final events in yeast exocytosis.* J Cell Biol, 2000. **151**(2): p. 439-451.

67. Bucci, C., R.G. Parton, I.H. Mather, H. Stunnenberg, K. Simons, B. Hoflack, and M. Zerial, *The small GTPase rab5 functions as a regulatory factor in the early endocytic pathway.* Cell, 1992. **70**: p. 715-728.

68. Barbieri, M.A., S. Hoffenberg, R. Roberts, A. Mukhopadhyay, A. Pomrehn, B.F. Dickey, and P.D. Stahl, *Evidence for a symmetrical requirement for Rab5-GTP in in vitro endosome-endosome fusion.* J Biol Chem, 1998. **273**(40): p. 25850-25855.

69. Rybin, V., O. Ullrich, M. Rubino, K. Alexandrov, I. Sijmon, M.C. Seabra, R. Goody, and M. Zerial, *GTPase activity of Rab5 acts as a timer for endocytic membrane fusion.* Nature, 1996. **383**: p. 266-269.

70. Chiariello, M., C.B. Bruni, and C. Bucci, *The small GTPases Rab5a, Rab5b and Rab5c are differentially phosphorylated in vitro.* FEBS Lett, 1999. **453**(1-2): p. 20-24.

71. Nakamura, S., Y. Kawamoto, S. Nakano, and I. Akiguchi, *Expression of the endocytosis regulatory proteins Rab5 and Rabaptin-5 in glial cytoplasmic inclusions from brains with multiple system atrophy.* Clin Neuropathol, 2000. **19**(2): p. 51-56.

72. Rafaniello, R.D., J. Lin, and J.P. Raufman, *Actions and expression of RAB-GDP dissociation inhibitor in dispersed chief cells from guinea pig stomach.* Biochem Biophys Res Commun, 1996. **225**(1): p. 232-237.

73. Wagner, A.C.C., M.Z. Strowski, and J.A. Williams, *Identification of Rab 5 but not Rab 3A in rat pancreatic zymogen granule membranes.* Biochem Biophys Res Commun, 1994. **200**(1): p. 542-548.

74. Ullrich, O., S. Reinsch, S. Urbe, M. Zerial, and R.G. Parton, *Rab11 regulates recycling through the pericentriolar recycling endosome.* J Cell Biol, 1996. **135**(4): p. 913-924.

75. Kessler, A., E. Tomas, D. Immler, H.E. Meyer, A. Zorzano, and J. Eckel, *Rab11 is associated with GLUT4-containing vesicles and redistributes in response to insulin.* Diabetologia, 2000. **43**: p. 1518-1527.

76. Chen, W., Y. Feng, D. Chen, and A. Wandinger-Ness, *Rab11 is required for trans-Golgi network-to-plasma membrane transport and a preferential target for GDP dissociation inhibitor.* Mol Biol Cell, 1998. **9**: p. 3241-3257.

77. Wilcke, M., L. Johannes, T. Galli, V. Mayau, B. Goud, and J. Salmero, *Rab11 regulates the compartmentalization of early endosomes required for efficient transport from early endosomes to the trans-Golgi network.* J Cell Biol, 2000. **151**(6): p. 1207-1220.

78. Kikuchi, A., T. Yamashita, M. Kawata, K. Yamamoto, K. Ikeda, T. Tanimoto, and Y. Takai, *Purification and characterization of a novel GTP-binding protein with a molecular weight of 24,000 from bovine brain membranes.* J Biol Chem, 1988. **263**(6): p. 2897-2904.

79. Chavrier, P., M. Vingron, C. Sander, K. Simons, and M. Zerial, *Molecular cloning of YPT1/SEC4-related cDNAs from an epithelial cell line.* Mol Cell Biol, 1990. **10**(12): p. 6578-6585.

80. Goldenring, J.R., C.J. Soroka, K.R. Shen, L.H. Tang, W. Rodriguez, H.D. Vaughan, S.A. Stoch, and I.M. Modlin, *Enrichment of rab11, a small GTP-binding protein, in gastric parietal cells.* Am J Physiol, 1994. **267**(2 Pt 1): p. G187-G194.

81. Lai, F., L. Stubbs, and K. Artzt, *Molecular analysis of mouse Rab11b: a new type of mammalian YPT/Rab protein.* Genomics, 1994. **22**(3): p. 610-616.

82. Calhoun, B.C., L.A. LaPierre, C.S. Chew, and J.R. Goldenring, *Rab11a redistributes to apical secretory canaliculus during stimulation of gastric parietal cells.* Am J Physiol, 1998. **275**: p. C163-C170.

83. Duman, J.G., K. Tyagarajan, M.S. Kolsi, H.H. Moore, and J.G. Forte, *Expression of rab11aN124I in gastric parietal cells inhibits stimulatory recruitment of the H^+-K^+-ATPase.* Am J Physiol, 1999. **277**: p. C361-C372.

84. Zhao, H. and K. Vaananen. *Rab11 is associated with pericentriolar recycling compartment in multinuclear osteoclasts.* in *American Society of Cell Biology.* 1998. San Francisco CA.

85. Ray, G.S., J.R. Lee, K. Nwokeji, L.R. Mills, and J.R. Goldenring, *Increased immunoreactivity for Rab11, a small GTP-binding protein, in low-grade dysplastic Barrett's epithelia.* Lab Invest, 1997. **77**(5): p. 503-511.

86. Chen, D., P. Ganapathy, L.J. Zhu, X. Xu, Q. Li, I.C. Bagchi, and M.K. Bagchi, *Potential regulation of membrane trafficking by estrogen receptor alpha via induction of rab11 in uterine glands during implantation.* Mol Endocrinol, 1999. **13**(6): p. 993-1004.

87. Goldenring, J.R., J. Smith, H.D. Vaughan, P. Cameron, W. Hawkins, and J. Navarre, *Rab11 is an apically located small GTP-binding protein in epithelial tissues.* Am J Physiol, 1996. **270**: p. G515-G525.

88. Zahraoui, A., G. Joberty, M. Arpin, J.J. Fontaine, R. Hellio, A. Tavitian, and L. D, *A small rab GTPase is distributed in cytoplasmic vesicles in non polarized cells but colocalizes with the tight junction marker ZO-1 in polarized epithelial cells.* J Cell Biol, 1994. **124**(1 and 2): p. 101-115.

89. Lütcke, A., R.G. Parton, C. Murphy, V.M. Olkkonen, P. Dupree, A. Valencia, K. Simons, and M. Zerial, *Cloning and subcellular localization of novel rab proteins reveals polarized and cell type-specific expression.* J Cell Sci, 1994. **107**(3437-3448).

90. Schafer, U., S. Seibold, A. Schneider, and E. Neugebauer, *Isolation and characterization of the human rab18 gene after stimulation of endothelial cells with histamine.* FEBS Lett, 2000. **466**: p. 148-154.

91. Bao, S., J. Zhu, and W.T. Garvey, *Cloning of Rab GTPases expressed in human skeletal muscle: studies in insulin-resistant subjects.* Horm Metab Res, 1998. **30**(11): p. 656-662.

92. Shiraishi, F., L.M. Curtis, L. Truong, K. Poss, G.A. Visner, K. Madsen, H.S. Nick, A. Agarwal, and R. Gottlieb, *Heme oxygenase-1 gene ablation or expression modulates cisplatin-induced renal tubular apoptosis.* Am J Physiol Renal Physiol, 2000. **278**(5): p. F726-F736.

93. Gavrielli, Y., Y. Sherman, and S.A. Ben-Sasson, *Identification of programmed cell death in situ via specific labeling of nuclear DNA fragmentation.* J Cell Biol, 1992. **119**: p. 493-501.

94. Hemken, P., X.-L. Guo, Z.-Q. Wang, K. Zhang, and S. Gluck, *Immunologic evidence that vacuolar H^+ ATPases with heterogeneous forms of M_r=31,000 subunit have different membrane distributions in mammalian kidney.* J Biol Chem, 1992. **267**(14): p. 9948-9957.

95. Linser, P.J., M. Sorrentino, and A.A. Moscana, *Cellular compartmentalization of carbonic anhydrase-C and glutamine synthetase in develooping and mature mouse neural retina.* Dev Brain Res, 1984. **13**: p. 65-71.

96. Kim, J., C.C. Tisher, P.J. Linser, and K.M. Madsen, *Ultrastructural localization of carbonic anhydrase II in subpopulations of intercalated cells of the rat kidney.* J Am Soc Nephrol, 1990. **1**: p. 245-256.

97. Ausubel, F.M., R. Brent, R.E. Kingston, D.D. Moore, J.G. Seidman, J.A. Smith, and K. Struhl, eds. *Current Protocols in Molecular Biology.* 1994, John Wiley & Sons, Inc: New York, NY.

98. Tsuchida, S., T. Matsusaka, X. Chen, S. Okubo, F. Niimura, H. Nishimura, A. Fogo, H. Utsunomiya, T. Inagami, and I. Ichikawa, *Murine double nullizygotes of the angiotensin type 1A and 1B receptor genes duplicate severe abnormal phenotypes of angiotensinogen nullizygotes.* J Clin Invest, 1998. **101**(4): p. 755-760.

99. Nishimura, J., T. Matsusaka, H. Utsunomiya, A. Fogo, V. Kon, T. Inagami, and I. Ichikawa, *Gene targeting reveals that angiotensin type 2 receptor (AT2) is not essential for embryonic development of the kidney.* J Am Soc Nephrol, 1996. **7**: p. 1602.

100. Ma, J., H. Nishimura, A. Fogo, V. Kon, T. Inagami, and I. Ichikawa, *Accelerated fibrosis and collagen deposition develop in the renal interstitium of angiotensin type 2 receptor null mutant mice during ureteral obstruction.* Kidney Int, 1998. **53**: p. 937-944.

101. Maric, C., G.P. Aldred, P.J. Harris, and D. Alcorn, *Angiotensin II inhibits growth of cultured embryonic renomedullary interstitial cells through the AT_2 receptor.* Kidney Int, 1998. **53**: p. 92-99.

102. Nishimura, H., E. Yerkes, M. Schulman, A. Fogo, V. Kon, B.L.M. Hogan, J.A.I. Phillips, J.W. Brock, T. Inagami, and I. Ichikawa, *Null mutation of the murine angiotensin type 2 receptor gene produces a spectrum of phenotypes resembling human congenital urinary tract anomalies (CUTA).* J Am Soc Nephrol, 1997. **8**: p. 364A.

103. Tufro-McReddie, A., L.M. Romano, J.M. Harris, L. Ferder, and R.A. Gomez, *Angiotensin II regulates nephrogenesis and renal vascular development.* Am J Physiol, 1995. **269**: p. F110-F115.

104. Kinoshita, K., T. Waritani, M. Noto, K. Takizawa, Y. Minemoto, A. Nishikawa, and S. Ohkuma, *Bafilomycin A1 induces apoptosis in PC12 cells independently of intracellular pH.* FEBS Lett, 1996. **398**(1): p. 61-66.

105. Dumanchin, C., C. Czech, D. Campion, M.H. Cuif, T. Poyot, C. Martin, F. Charbonnier, B. Goud, L. Pradier, and T. Frebourg, *Presenilins interact with Rab11, a small GTPase involved in the regulation of vesicle transport.* Hum Mol Genet, 1999. **8**(7): p. 1263-1269.

106. Echevarria, O.M., A. Gonzalez Maciel, A.M. Traish, H.H. Wotiz, E. Ubaldo, and G.H. Vazquez-Nin, *Immuno-electron microscopic localization of estradiol receptor in cells of male and female reproductive and non-reproductive organs.* Biol Cell, 1994. **81**(3): p. 257-265.

107. Verlander, J.W., T.M. Tran, L. Zhang, M.R. Kaplan, and S.C. Hebert, *Estradiol enhances thiazide-sensitive NaCl cotransporter density in the apical plasma membrane of the distal convoluted tubule in ovariectomized rats.* J Clin Invest, 1998. **101**(8): p. 1661-1669.

108. Quamme, G., *Control of magnesium transport in the thick ascending limb.* Am J Physiol, 1989. **256**: p. F197-F210.

109. Schwartz, J.H., S.A. Masino, R.D. Nichols, and E.A. Alexander, *Intracellular modulation of acid secretion in rat inner medullary collecting duct cells.* Am J Physiol, 1994. **266**((1 Pt 2)): p. F94-101.

110. Alexander, E.A., D. Brown, T. Shih, M. McKee, and J.H. Schwartz, *Effect of acidification on the location of H+-ATPase in cultured inner medullary collecting duct cells.* Am J Physiol, 1999. **276**((3 Pt 1)): p. C758-63.

111. Banerjee, A., T. Shih, E.A. Alexander, and J.H. Schwartz, *SNARE proteins regulate H(+)-ATPase redistribution to the apical membrane in rat renal inner medullary collecting duct cells.* J Biol Chem, 1999. **274**(37): p. 26518-22.

112. Banerjee, A., G. Li, E.A. Alexander, and J.H. Schwartz, *Role of SNAP-23 in trafficking of H+-ATPase in cultured inner medullary collecting duct cells.* Am J Physiol Cell Physiol, 2001. **280**(4): p. C775-81.

BIOGRAPHICAL SKETCH

Lisa M. Curtis received her Associate of Arts degree in 1983 from St. Petersburg Junior College where she was listed on the Dean's List for several semesters. She received a Bachelor of Science degree in microbiology and cell science in 1988 and a second Bachelor of Science degree in chemistry in 1990, both from the University of Florida. She then worked in the laboratories of Dr. Kyle Rarey in the Department of Anatomy and Cell Biology at the University of Florida as a Biological Scientist (1990-1993) and Senior Biological Scientist (1993-1995). She entered the cell and developmental biology graduate program in the Department of Anatomy and Cell Biology in the Fall of 1995. During her graduate program, she worked with Dr. Kirsten Madsen in the Division of Nephrology, University of Florida, to examine the role of angiotensin II in developmental apoptosis in the kidney, for which she was the recipient of a two-year Graduate Student Fellowship Award from the American Heart Association, Florida Affiliate in 1998. She continued her graduate work with Dr. Stephen Gluck in the Division of Nephrology, University of Florida, to identify small GTP-binding proteins that associate with the vacuolar proton pump. She is an author on over 25 publications and abstracts resulting from her work with Dr. Rarey prior to graduate school and from her work with Drs. Madsen and Gluck during her graduate program. She intends to pursue an academic position with a focus on cancer cell biology.

I certify that I have read this study and that in my opinion it conforms to acceptable standards of scholarly presentation and is fully adequate, in scope and quality, as a dissertation for the degree of Doctor of Philosophy.

Stephen L. Gluck, Chair
Professor of Anatomy and Cell Biology

I certify that I have read this study and that in my opinion it conforms to acceptable standards of scholarly presentation and is fully adequate, in scope and quality, as a dissertation for the degree of Doctor of Philosophy.

Kirsten M. Madsen
Associate Professor of Anatomy and Cell Biology

I certify that I have read this study and that in my opinion it conforms to acceptable standards of scholarly presentation and is fully adequate, in scope and quality, as a dissertation for the degree of Doctor of Philosophy.

Stephen Sugrue
Associate Professor of Anatomy and Cell Biology

I certify that I have read this study and that in my opinion it conforms to acceptable standards of scholarly presentation and is fully adequate, in scope and quality, as a dissertation for the degree of Doctor of Philosophy.

Jill Verlander Reed
Associate Scientist of Anatomy and Cell Biology

I certify that I have read this study and that in my opinion it conforms to acceptable standards of scholarly presentation and is fully adequate, in scope and quality, as a dissertation for the degree of Doctor of Philosophy.

John Aris
Associate Professor of Anatomy and Cell Biology

I certify that I have read this study and that in my opinion it conforms to acceptable standards of scholarly presentation and is fully adequate, in scope and quality, as a dissertation for the degree of Doctor of Philosophy.

Susan R. Frost

Susan Frost
Professor of Biochemistry and
Molecular Biology

This dissertation was submitted to the Graduate Faculty of the College of Medicine and to the Graduate School and was accepted as partial fulfillment of the requirements for the degree of Doctor of Philosophy.

December, 2001

Wayne J. McCormack

Dean, College of Medicine

Dean, Graduate School

UNIVERSITY OF FLORIDA
3 1262 08555 2650